Scientific Report No. 91

A GENERALIZED EDGE BOUNDARY CONDITION FOR OPEN MICROSTRIP STRUCTURES

by

Thomas M. Martinson and Edward F. Kuester

Electromagnetics Laboratory
Department of Electrical and Computer Engineering
University of Colorado
Boulder, Colorado 80309

August 1987

This research was supported by the U.S. Office of Naval Research (ONR) under Contract No. N00014-86-K-0417.

ABSTRACT

A generalized edge boundary condition (GEBC) relating the tangential electric and magnetic fields at the edge of an arbitrarily shaped microstrip patch antenna on thin substrate is developed. This boundary condition incorporates the dynamical edge effects and the coupling over the patch. Based on this edge condition, commonly used microstrip patches can be accurately and efficiently analyzed. Using perturbation theory, resonant frequencies and Q-factors can be readily determined for simple patch shapes. Rectangular and circular microstrip antennas are analyzed in detail, and calculated results are compared with previously published experimental data.

1. INTRODUCTION

In the last decade, many analysis techniques have been applied to microstrip patch antennas. Numerical approaches such as full-wave analysis [1], and direct solution of the exact integral equation for the patch current [2]-[5] can provide the needed accuracy for many designs. However, lengthy computing times limit the applicability of such numerical techniques. On the other hand, models relying strongly on the physics of the problem, such as the transmission line model [6]-[8] and the cavity model [9]-[11], have been extensively used for simple patch shapes. In these two models, fields are reckoned under the patch and obey a transmission-line equation and a two-dimensional Helmholtz equation respectively. One of the main difficulties faced by these simple analysis techniques, is the accurate determination of the condition that the field must satisfy at the edge of the patch. This boundary condition, directly related to the fringing of the field, plays a crucial role in the accuracy of the analysis.

We will develop here a generalized edge boundary condition (GEBC) at the edge of an arbitrarily shaped microstrip patch antenna on electrically thin substrate ($kd<<1$). This boundary condition will include the effects of the coupling over the patch, radiation waves and surface waves.

First we set up an aperture field integral relation (AFIR) in the region extending from the edge of the patch to infinity at the air-dielectric interface. Second, we derive an integral expression for the tangential magnetic field at the edge of the patch and combine this relation with the AFIR. Third, the field distribution close to the edge is approximated by an equivalent static distribution multiplied by an amplitude factor dependent on position along the edge. Finally, we accurately approximate the kernel of our integral relation so as to isolate known static field integrals. The result is an expression for the tangential magnetic field at a given point along the edge as a function of the tangential magnetic field and the vertical electric field around the patch. This expression, or GEBC, allows two interesting applications. First, we derive a segmented version of the GEBC, useful for the analysis of arbitrarily shaped microstrip patches. Second, we develop a perturbation approach to analyze efficiently and accurately simple patch resonators. The time convention $e^{i\omega t}$ is used throughout.

2. APERTURE FIELD INTEGRAL RELATION

In contrast to most integral equation formulations [2]-[5], that set up an integral equation on the surface of the patch, we will derive an aperture field integral relation (AFIR) at the air-dielectric interface away from the patch. This approach bears some resemblance with one used a few years ago by Butler for the circular patch [12].

Consider the geometry of an arbitrarily shaped patch antenna illustrated in Fig. 1. A local coordinate system $(\vec{a}_n, \vec{a}_l, \vec{a}_z)$ is introduced everywhere along the edge of the patch. Let also S_C denote the surface of the conducting patch and S_A denote the aperture surface complement of S_C at z=d.

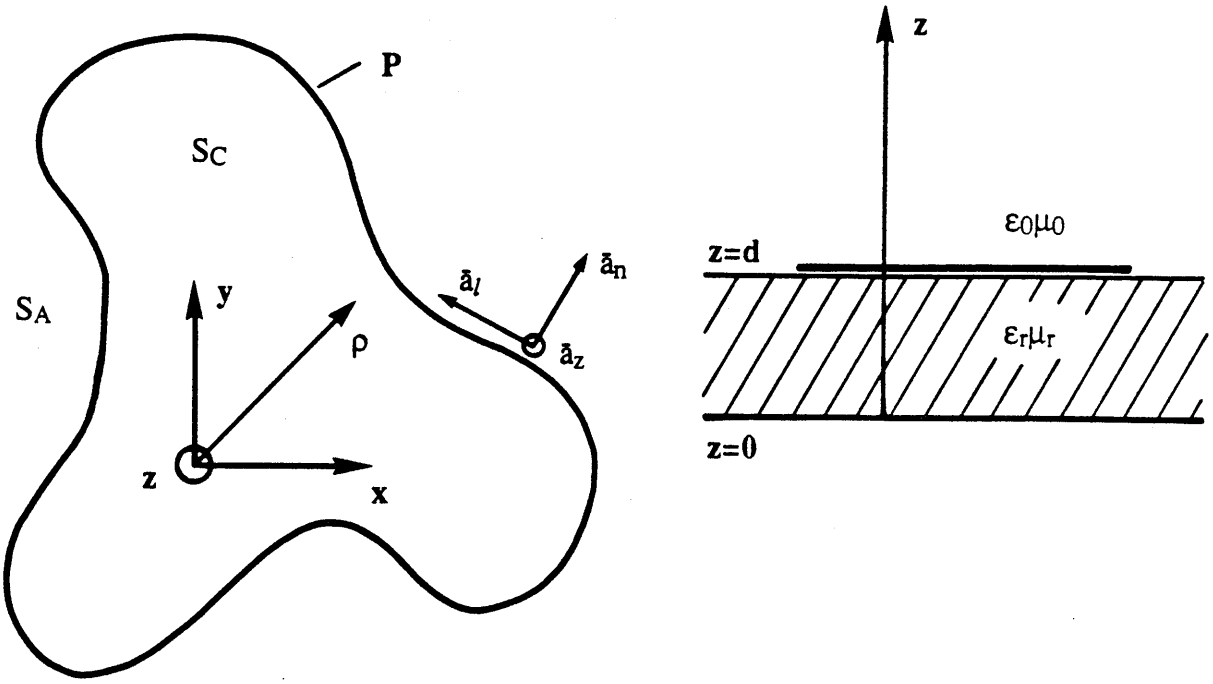

Top view **Side View**

Fig. 1. Arbitrarily shaped microstrip patch.

In a homogeneous source-free region, let G be the Green function solution of

$$[\nabla^2 + k^2]\, G = -\delta(\bar{r} - \bar{r}') \tag{1}$$

where $k = k_0(\epsilon_r \mu_r)^{1/2}$ and $k_0 = \omega(\epsilon_0 \mu_0)^{1/2}$ is the free space wavenumber. Let $\bar{c}$ be any constant vector. If we denote the scattered magnetic field by $\bar{H}^s$, we have the following integral relation, variant of a formula given by Harrington [13]:

$$\bar{c} \cdot \bar{H}^s(\bar{r}) = -\oint_S d\bar{s}' \cdot \left\{ \bar{H}^s \times (\nabla' \times \bar{c}G) - \bar{c}G \times (\nabla' \times \bar{H}^s) + \bar{H}^s(\nabla' \cdot \bar{c}G) \right\} \tag{2}$$

Since $\bar{c}$ is a constant vector:

$$\nabla \times G\bar{c} = \nabla G \times \bar{c}$$

$$\nabla \cdot G\bar{c} = \bar{c} \cdot \nabla G$$

Also, the corresponding source-free Maxwell equation gives the curl of the magnetic field:

$$\nabla' \times \bar{H}^s = i\omega\epsilon_0\epsilon_r \bar{E}^s$$

We therefore write directly

$$\bar{c} \cdot \bar{H}^s(\bar{r}) = \oint_S d\bar{s}' \cdot \left\{ (\bar{H}^s \times (\bar{c} \times \nabla' G) + i\omega\epsilon_0\epsilon_r G(\bar{c} \times \bar{E}^s) - \bar{H}^s(\bar{c} \cdot \nabla' G) \right\} \quad (3)$$

We also can expand

$$\bar{H}^s \times (\bar{c} \times \nabla' G) = (\bar{H}^s \cdot \nabla' G)\bar{c} - (\bar{H}^s \cdot \bar{c})\nabla' G$$

and thus (3) becomes

$$\bar{c} \cdot \bar{H}^s(\bar{r}) =$$

$$\oint_S d\bar{s}' \cdot \left\{ (\bar{H}^s \cdot \nabla' G)\bar{c} - (\bar{H}^s \cdot \bar{c})\nabla' G + i\omega\epsilon_0\epsilon_r G(\bar{c} \times \bar{E}) - \bar{H}^s(\bar{c} \cdot \nabla' G) \right\} \quad (4)$$

We will now use this integral relation to derive expressions for the tangential magnetic field on both sides of the air-dielectric interface. Let's indicate the air region (z>d) by the subscript 1 and the dielectric region (0<z<d) by the subscript 2, as shown in Fig. 2. The volume V_1 occupies the entire half-space above the patch, its boundary S_1 receding to infinity. The volume V_2 encloses the entire dielectric slab, the lateral sides of its boundary S_2 also receding to infinity.

In the region 1 (z>d), we define a Green function G_1 as follows

$$[\nabla^2 + k_0^2] G_1 = -\delta(\bar{r} - \bar{r}') \quad (5)$$

along with a Neumann boundary condition on the interface plane:

$$\frac{\partial G_1}{\partial z}\Big|_{z=d} = 0 \qquad ; \qquad \forall\, \bar{\rho} \quad (6)$$

Appendix A gives the well-known result:

$$G_1 = \frac{1}{4\pi}$$

$$\cdot \left[\frac{e^{-ik_0\left((x-x')^2 + (y-y')^2 + (z-z')^2\right)^{1/2}}}{\left((x-x')^2 + (y-y')^2 + (z-z')^2\right)^{1/2}} + \frac{e^{-ik_0\left((x-x')^2 + (y-y')^2 + (z+z'-2d)^2\right)^{1/2}}}{\left((x-x')^2 + (y-y')^2 + (z+z'-2d)^2\right)^{1/2}} \right] \quad (7)$$

Replacing G by G_1 and S by S_1 in (4), we can discard the portion of S_1 at infinity, since

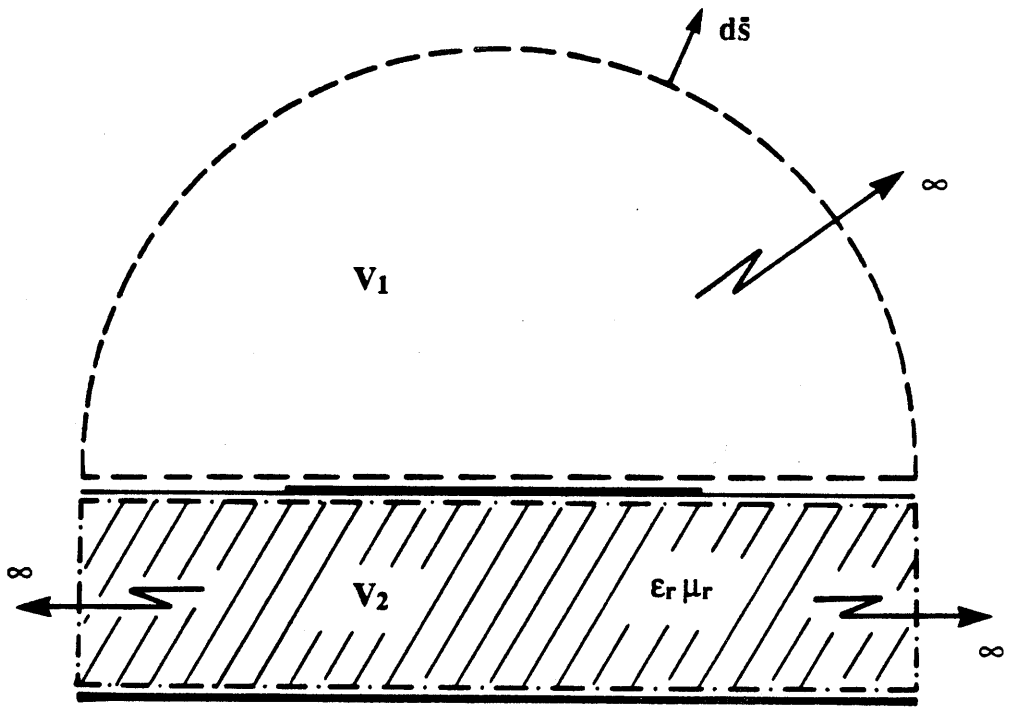

Fig. 2. Volumes V_1 and V_2 for application of Green's theorem.

$$G_1 = O(e^{Im[k_0]\,|\bar{r}-\bar{r}'|}/|\bar{r}-\bar{r}'|) \qquad as\ |\bar{r}-\bar{r}'| \to \infty \quad in\ V_1 \tag{8}$$

and we can apply the limiting absorption principle. Thus,

$$\bar{c}\cdot\bar{H}^t(\bar{r}_1) =$$

$$\int_{S_C+S_A} d\bar{s}'\cdot\left\{(\bar{H}^t\cdot\nabla' G_1)\bar{c} - (\bar{H}^t\cdot\bar{c})\nabla' G_1 + i\omega\epsilon_0 G_1(\bar{c}\times\bar{E}^t) - \bar{H}^t(\bar{c}\cdot\nabla' G_1)\right\}$$

with $d\bar{s}' = -\,\bar{a}_z' ds'$ and $z' = d^+$. Now, we choose the arbitrary constant vector $\bar{c}$ as any vector in the z=d plane. Then, enforcing the boundary condition (6):

$$\bar{H}_t^t(\bar{r}_1) = \int_{S_C+S_A} ds'\left\{H_z^t\nabla' G_1 - i\omega\epsilon_0 G_1(\bar{E}^t\times\bar{a}_z')\right\}$$

where $\bar{H}_t^t$ is the projection of $\bar{H}^t$ in the plane $z = d^+$. Since the surface of the patch is perfectly electrically conducting

$$\bar{E}^s \times \bar{a}_z \Big|_{S_c} = 0$$

$$H_z^s \Big|_{S_c} = 0$$

We can finally write

$$\bar{H}_t^s(\bar{r}_1) = \int_{S_A} ds' \left\{ H_z^s \nabla' G_1 - i\omega\epsilon_0 G_1 (\bar{E}^s \times \bar{a}_z') \right\} \quad ; \quad z' = d^+ \tag{9}$$

where $\bar{r}_1 \in V_1$. In the region 2 (0<z<d), we define a Green function G_2 as follows

$$[\nabla^2 + k^2] G_2 = -\delta(\bar{r} - \bar{r}') \tag{10}$$

with a Neumann boundary condition on the interface plane $z = d$ and the ground plane $z = 0$

$$\frac{\partial G_2}{\partial z} \Big|_{z=0,d} = 0 \quad ; \quad \forall \bar{\rho} \tag{11}$$

Appendix A gives the well-known result:

$$G_2 = G_2^c + G_2^{TEM} \tag{12a}$$

with

$$G_2^c = -\frac{i}{2d} \sum_{m=1}^{\infty} \cos\frac{m\pi z}{d} \cos\frac{m\pi z'}{d} \; \mathbf{H}_0^{(2)} \left(\left(k^2 - \frac{m^2\pi^2}{d^2}\right)^{1/2} |\bar{\rho} - \bar{\rho}'| \right) \tag{12b}$$

$$G_2^{TEM} = -\frac{i}{4d} \mathbf{H}_0^{(2)} (k\,|\bar{\rho} - \bar{\rho}'|) \tag{12c}$$

where $\mathbf{H}_0^{(2)}$ is the Hankel function of the second kind of order 0 and the branch of the square root is given as

$$\left(k^2 - \frac{m^2\pi^2}{d^2}\right)^{1/2} = -i\left(\frac{m^2\pi^2}{d^2} - k^2\right)^{1/2} \tag{13}$$

Also, as source and observation points move apart, G_2 behaves as

$$G_2 = \mathrm{O}\left(e^{Im[k]|\bar{\rho} - \bar{\rho}'|} \Big/ |\bar{\rho} - \bar{\rho}'|^{1/2}\right) \quad as \; |\bar{\rho} - \bar{\rho}'| \to \infty \; in \; V_2$$

so that we can discard the contribution of S_2 at infinity. Following closely the derivation of (9), we get a similar expression for the horizontal magnetic field in region 2:

$$\bar{H}_t^s(\bar{r}_2) = -\int_{S_A} ds' \left\{ H_z^s \nabla' G_2 - i\omega\epsilon_0\epsilon_r G_2 (\bar{E}^s \times \bar{a}_z') \right\} \quad ; \quad z' = d^- \tag{14}$$

Consider an incident TEM field under the patch. This field corresponds to the dominant mode of the corresponding parallel-plate waveguide. We assume its presence everywhere in the dielectric slab:

$$\bar{E}^i = \bar{a}_z E_z^i(\bar{\rho})$$
$$\bar{H}^i = \bar{a}_z H_z^i(\bar{\rho}) + \bar{a}_y H_y^i(\bar{\rho}) \qquad \forall\, \bar{\rho} \;;\; 0<z<d \tag{15}$$

We note that the incident field satisfies the boundary conditions on the top patch and on the ground plane. At the edge of the patch, the normal surface electric current or, equivalently, the discontinuity of the total tangential magnetic field must vanish:

$$\bar{a}_l \cdot \left\{ \bar{H}_l^i(n=0,l,z=d^+) - \bar{H}_l^i(n=0,l,z=d^-) - \bar{H}_l^i(n=0,l,z=d^-) \right\} = 0 \tag{16}$$

Replacing $\bar{H}_l^i$ by the integral expressions developed above, (9) and (14), we obtain an important aperture integral relation:

$$H_l^i(n=0,l,z=d^-) =$$
$$\bar{a}_l \cdot \int_{S_A} ds' \left[H_z(n',l') [\nabla' G_1 + \frac{\nabla' G_2}{\mu_r}] - i\omega\epsilon_0 [\bar{E}(n',l') \times \bar{a}_z'] [G_1 + \epsilon_r G_2] \right] \tag{17}$$

where

$$G_1 = G_1(n=0,l,z=d\,;n',l',z'=d)$$
$$G_2 = G_2(n=0,l,z=d\,;n',l',z'=d)$$
$$H_z(n',l') = H_z(n',l',z'=d^+)$$

3. TANGENTIAL MAGNETIC FIELD AT THE EDGE OF THE PATCH

Our next step will give an integral expression for the tangential TEM part of the scattered magnetic field under the patch. This TEM component corresponds to the dominant modes we want to excite under the patch. Equation (14) yields at once

$$H_l^{TEM,s}\,(n=0,l,z=d^-) =$$
$$\bar{a}_l \cdot \int_{S_A} ds' \left\{ - H_z(n',l') \frac{\nabla' G_2^{TEM}}{\mu_r} + i\omega\epsilon_0\epsilon_r G_2^{TEM} [\bar{E}\,(n',l') \times \bar{a}_z'] \right\} \tag{18}$$

where the kernel G_2^{TEM} is given by (12c). As it stands now, (18) is an exact relation. But, since we do not know the field components H_z and $(\bar{E} \times \bar{a}_z)$ in the aperture S_A, this equation is not directly useful. The strategy here consists of finding a suitable static approximation for the field in the aperture region. However, If we were to introduce these approximations in equation (18) directly, the resulting approximation for H_l^{TEM} would likely be inaccurate. Following a scheme successfully applied earlier in a similar problem [14], we combine (18) with the integral form of the edge condition (17). Then, the approximation of the aperture field by quantities proportional to the corresponding static distribution will

give us accurate results.

Recalling the edge condition (17) and denoting the total tangential TEM magnetic field by $H_l^{TEM} = H_l^{TEM,s} + H_l^i$, (18) becomes

$$H_l^{TEM}\,(n=0,l,z=d^-) =$$

$$\bar{a}_l \cdot \int_{S_A} ds' \left\{ H_z(n',l')\,[\nabla' G_1 + \frac{\nabla' G_2^c}{\mu_r}] - i\omega\epsilon_0\,[\bar{E}(n',l') \times \bar{a}_z'][G_1 + \epsilon_r G_2^c] \right\} \quad (19)$$

In order to justify the approximations we will use for the aperture fields, we need to stress a few points. First H_l^{TEM} is a small quantity around the patch. Indeed, "ideal" cavity models set this component of the magnetic field to zero along the edge. Second, we must see that the dominant contribution in the right-hand side of (19) comes from a narrow region close to the edge because of the fast decay of the aperture field away from the edge. Third, the surface wave and radiation wave contribution are accounted for by the corresponding kernels, even if the aperture fields are not accurately approximated away from the edge. To approximate the true electric aperture field in the integral expression (19), we assume that the field emerges perpendicularly from the locally "straight" edge of the patch. Thus the dynamic field contribution can be adequately modelled by the product of a voltage V(l) dependent on position along the edge and the static field distribution $E_{0n}(n)$:

$$\bar{E} \times \bar{a}_z \simeq -\bar{a}_l E_{0n}(n)\,\frac{V(l)}{[1+n\chi(l)]} \quad (20)$$

where $\chi(l)$ is the curvature of the perimeter P at the point (n=0,l). The denominator of (20) takes care of the spreading of the field lines . The surface integral transformation is thus given by

$$ds = dn\,dl\,[1 + n\chi(l)] \quad (21)$$

To uniquely specify the static edge voltage, we enforce the following normalization:

$$\int_0^\infty dn'\,E_{0n}(n') = 1 \quad (22)$$

We can make a similar argument for the z-directed component of the aperture magnetic field, product of an amplitude factor $W(l)$ dependent on position along the edge and the static field distribution $H_{0z}(n)$ at $z=d^+$:

$$H_z \simeq H_{0z}(n)\frac{W(l)}{[1 + n\chi(l)]} \quad (23)$$

with a corresponding normalization:

$$\int_0^\infty dn'\,H_{0z}(n') = 1 \quad ; \quad z=d^+ \quad (24)$$

Although the static fields E_{0n} and H_{0z} stem from uncoupled static problems, the dynamical behavior of the field imposes a relationship between the amplitude factors V(l) and W(l). Faraday's equation applied at the locally "straight" edge yields

$$-i\omega\mu_0 H_z = \frac{\partial E_l}{\partial n} - \frac{\partial E_n}{\partial l} \quad ; \quad z = d^+ \tag{25}$$

Introducing the field approximations (20) and (23) into (25)

$$-i\omega\mu_0 W(l) H_{0z}(n) = [1 + n\chi(l)]\frac{\partial E_l}{\partial n} - E_{0n}(n)\frac{\partial V(l)}{\partial l} \quad ; \quad z = d^+$$

Integrating both sides of the above relation with respect to n from the edge to infinity, we get

$$-i\omega\mu_0 W(l) \int_0^\infty dn\, H_{0z}(n) = -\frac{\partial V(l)}{\partial l} \int_0^\infty dn\, E_{0n}(n) \quad ; \quad z = d^+ \tag{26}$$

where we have used both radiation condition $E_l(n \to \infty) = 0$ and the perfectly conducting edge condition $E_l(n = 0) = 0$. Recall the static field normalizations (22) and (24) to obtain

$$W(l) = -\frac{i}{\omega\mu_0}\frac{\partial V(l)}{\partial l} \tag{27}$$

We can now put the pieces together and write down the approximate expression for the TEM part of the tangential magnetic field at the edge:

$$H_l^{TEM}(n = 0, l, z = d^-) = \bar{a}_l \int_0^\infty dn' \oint_P dl'$$

$$\cdot \left[\frac{-i}{\omega\mu_0}\frac{\partial V}{\partial l'} H_{0z}(n')[\nabla' G_1 + \frac{\nabla' G_2^c}{\mu_r}] + i\omega\epsilon_0 \bar{a}_l' V(l') E_{0n}(n')[G_1 + \epsilon_r G_2^c] \right] \tag{28}$$

with

$$G_1 = \frac{1}{2\pi}\left\{ \frac{e^{-ik_0|\bar{\rho} - \bar{\rho}'|}}{|\bar{\rho} - \bar{\rho}'|} \right\}$$

$$G_2^c = -\frac{i}{2d} \sum_{m=1}^{\infty} \mathbf{H}_0^{(2)}\left((k^2 - \frac{m^2\pi^2}{d^2})^{1/2} |\bar{\rho} - \bar{\rho}'| \right)$$

4. GENERALIZED EDGE BOUNDARY CONDITION

Although the static field is known exactly from a Wiener-Hopf solution of the edge problem [15],[16], the integral relation (28) still does not prove very useful. The two-dimensional integration domain is infinite along one direction and the calculation of the static field requires computing a Laplace-transform integral [15]. This makes the evaluation of equation (28) very inefficient. One of the key features of the technique presented here is that the infinite integral can be approximated very accurately in closed form, making the result a function of a perimeter integral only.

For convenience, define a function $\Lambda(l)$ on the perimeter of the patch. We require $\Lambda(l)$ to be a smooth function of the edge coordinate l. By smooth, we mean

$$\Lambda(l+\delta) \simeq \Lambda(l)$$

where δ is a small distance of the order of a few d. We first form an inner product between expression (28) and $\Lambda(l)$ over the perimeter P:

$$\oint_P dl\,\Lambda(l) H_l^{TEM}\,(n=0,l,z=d^-) = \oint_P dl\,\Lambda(l)\,\bar{a}_l \int_0^\infty dn' \oint_P dl'$$

$$\cdot \left[-\frac{i}{\omega\mu_0}\frac{\partial V}{\partial l'} H_{0z}(n')[\nabla' G_1 + \frac{\nabla' G_2^c}{\mu_r}] + i\omega\epsilon_0 \bar{a}_l{}' V(l') E_{0n}(n')[G_1 + \epsilon_r G_2^c] \right]$$

Assuming we can change the order of the primed and unprimed integrals, the right-hand side of the above equation can be treated as the sum of four terms:

$$\oint_P dl\,\Lambda(l) H_l^{TEM}\,(n=0,l,z=d^-) = R_{11} + R_{12} + R_{21} + R_{22} \tag{29}$$

where

$$R_{11} = i\omega\epsilon_0 \int_0^\infty dn' \oint_P dl'\; V(l') E_{0n}(n')\,\bar{a}_l{}' \cdot \oint_P dl\,\Lambda(l)\,\bar{a}_l G_1 \tag{30}$$

$$R_{12} = i\omega\epsilon_0\epsilon_r \int_0^\infty dn' \oint_P dl' V(l') E_{0n}(n')\,\bar{a}_l{}' \cdot \oint_P dl\,\Lambda(l)\,\bar{a}_l G_2^c \tag{31}$$

$$R_{21} = -\frac{i}{\omega\mu_0} \int_0^\infty dn' \oint_P dl' \frac{\partial V}{\partial l'} H_{0z}(n') \oint_P dl\,\Lambda(l)\,\bar{a}_l \cdot \nabla' G_1 \tag{32}$$

$$R_{22} = -\frac{i}{\omega\mu_0\mu_r} \int_0^\infty dn' \oint_P dl' \frac{\partial V}{\partial l'} H_{0z}(n') \oint_P dl\,\Lambda(l)\,\bar{a}_l \cdot \nabla' G_2^c \tag{33}$$

These four terms are evaluated in Appendix B:

$$R_{11} = \frac{i\omega\epsilon_0}{2\pi} \int_0^\infty dn' E_{0n}(n') \oint_P dl'\; V(l')\,\bar{a}_l{}' \cdot \oint_P dl\,\Lambda(l)\,\bar{a}_l \frac{e^{-ik_0(|\bar{\rho}-\bar{\rho}_0{}'|^2+d^2)^{1/2}}}{(|\bar{\rho}-\bar{\rho}_0{}'|^2+d^2)^{1/2}}$$

$$-\frac{i\omega\epsilon_0}{\pi} \int_0^\infty dn'\, E_{0n}(n') \ln\left(\frac{n'}{d}\right) \oint_P dl'\,\Lambda(l')\,V(l') \tag{34}$$

$$R_{12} = -\frac{i\omega\epsilon_0\epsilon_r}{\pi} \int_0^\infty dn'\, E_{0n}(n') \ln(1-e^{-\pi n'/d}) \oint_P dl'\,\Lambda(l')\,V(l') \tag{35}$$

$$R_{21} = \frac{i}{2\pi\omega\mu_0} \int_0^\infty dn'\, H_{0z}(n') \oint_P dl' \frac{\partial V}{\partial l'} \oint_P dl\,\Lambda(l) \frac{\partial}{\partial l}\left[\frac{e^{-ik_0(|\bar{\rho}-\bar{\rho}_0{}'|^2+d^2)^{1/2}}}{(|\bar{\rho}-\bar{\rho}_0{}'|^2+d^2)^{1/2}}\right]$$

$$-\frac{i}{\pi\omega\mu_0}\int_0^\infty dn' H_{0z}(n')\ln\left(\frac{n'}{d}\right)\oint_P dl'\Lambda(l')\frac{\partial^2 V}{\partial l'^2} \tag{36}$$

$$R_{22} = -\frac{i}{\pi\omega\mu_0\mu_r}\int_0^\infty dn' H_{0z}(n')\ln\left(1-e^{-\pi n'/d}\right)\oint_P dl'\Lambda(l')\frac{\partial^2 V}{\partial l'^2} \tag{37}$$

where $\bar{\rho}_0'(n'=0,l')$ is the projection of $\bar{\rho}'(n',l')$ on P as shown in Fig. B1. At this point, we recall two dual results on static field integrals derived in a previous report [14]. We must emphasize that these integrals, based on a Wiener-Hopf solution of the static straight edge problem, are exact.

$$\int_0^\infty dn' E_{0n}(n')\left[\ln\left(\frac{n'}{d}\right)+\epsilon_r\ln\left(1-e^{-\pi n'/d}\right)\right] = \ln 2 + 2\epsilon_r Q_0(-\delta_\epsilon) - \epsilon_r\ln(2\pi) - 1 \tag{38}$$

where

$$Q_0(x) = \sum_{m=1}^{\infty} x^m \ln m \tag{39}$$

and δ_ϵ is a dielectric contrast coefficient given by

$$\delta_\epsilon = \frac{\epsilon_r - 1}{\epsilon_r + 1} \tag{40}$$

Likewise,

$$\int_0^\infty dn' H_{0z}(n')\left[\ln\left(\frac{n'}{d}\right)+\frac{1}{\mu_r}\ln\left(1-e^{-\pi n'/d}\right)\right] = \ln 2 + \frac{2}{\mu_r}Q_0(\delta_\mu) - \frac{1}{\mu_r}\ln(2\pi) - 1 \tag{41}$$

where

$$\delta_\mu = \frac{\mu_r - 1}{\mu_r + 1} \tag{42}$$

If we substitute expressions (38) and (41) together with normalizations (22) and (24) into the four terms (34)-(37) and rearrange, then the boundary condition (29) becomes

$$\oint_P dl\,\Lambda(l)\,H_l^{TEM}(n=0,l,z=d^-) =$$

$$\frac{i\omega\epsilon_0}{2\pi}\oint_P dl'\,V(l')\,\bar{a}_{l'}\cdot\oint_P dl\,\Lambda(l)\,\bar{a}_l\,G_d(l,l') + \frac{i}{2\pi\omega\mu_0}\oint_P dl'\frac{\partial V}{\partial l'}\oint_P dl\,\Lambda(l)\frac{\partial}{\partial l}G_d(l,l')$$

$$-\frac{i\omega\epsilon_0}{\pi}F(\epsilon_r)\oint_P dl'\,\Lambda(l')\,V(l') - \frac{i}{\pi\omega\mu_0}F\left(\frac{1}{\mu_r}\right)\oint_P dl'\,\Lambda(l')\frac{\partial^2 V}{\partial l'^2} \tag{43}$$

where we have defined for convenience

$$F(x) = \ln 2 + 2x\,Q_0\left(\frac{1-x}{1+x}\right) - x\ln(2\pi) - 1 \tag{44}$$

and

$$G_d(l,l') = \frac{e^{-ik_0(|\bar{\rho} - \bar{\rho}_0'|^2 + d^2)^{1/2}}}{(|\bar{\rho} - \bar{\rho}_0'|^2 + d^2)^{1/2}} \quad | \quad \bar{\rho},\bar{\rho}_0' \in P \tag{45}$$

Equation (43) can be considered as the generic form of a generalized edge boundary condition (GEBC). The relative freedom we have in choosing $\Lambda(l)$ allows for several distinct applications. In the following sections, we will describe two such developments. First, segmenting the patch and letting $\Lambda(l)$ become a pulse function, we get a generalized boundary condition readily applicable to various microstrip structures, such as antennas and discontinuities. Second, letting $\Lambda(l) = V(l)$, the actual edge voltage, we can build a perturbation expression for the resonant frequencies and Q-factor of microstrip patch resonators.

Letting $\Lambda(l)$ become a sequence of functions approaching a Dirac impulse, we can write a "local form" of the GEBC:

$$H_l^{TEM}(n=0,l,z=d^-) = \frac{i\omega\epsilon_0}{\pi}\left\{ - F(\epsilon_r)\, V(l) + \frac{1}{2}\oint_P dl'\, V(l')[\bar{a}_l' \cdot \bar{a}_l] G_d(l,l') \right\}$$

$$+ \frac{i}{\pi\omega\mu_0}\left\{ - \frac{\partial^2 V(l)}{\partial l^2}\, F(\frac{1}{\mu_r}) + \frac{1}{2}\frac{\partial}{\partial l}\oint_P dl'\, \frac{\partial V}{\partial l'}\, G_d(l,l') \right\} \tag{46}$$

We have however to keep in mind that this expression is only valid, strictly speaking, when we take an inner product on both sides with a relatively smooth function $\Lambda(l)$. Nevertheless, this local form of the GEBC provides a convenient tool, with much physical insight.

5. SEGMENTATION OF THE PATCH

We represent an arbitrarily shaped patch by a succession of straight segments, as shown in Fig. 3. In order to provide as much generality as possible, the segments S_i can be of unequal lengths Δ_i. Furthermore, we assume that the number of segments is such that the shape of the patch is reasonably well approximated and that the edge voltage does not vary widely along one segment. We denote by $\bar{a}_{li}$ the unit vector tangent to the segment S_i. Also we indicate by $\bar{\rho}_i\,(n=0, l=l_i)$ the position vector of the segment's middle-point. Consistent with this segmentation, we let $\Lambda(l) = \Pi_i(l)$, where $\Pi_i(l)$ is a piecewise constant pulse function defined as follows

$$\Pi_i(l) = \begin{cases} 1 \;;\; l \in S_i \\ 0 \;;\; otherwise \end{cases}$$

Therefore, we can write a segmented version of the generalized boundary condition directly from expression (43):

$$H_l^{TEM}(l_i) = \frac{i\omega\epsilon_0}{2\pi\Delta_i}\oint_P dl'\, V(l')\, \bar{a}_l' \cdot \int_{S_i} dl\, \bar{a}_{li}\, G_d(l,l')$$

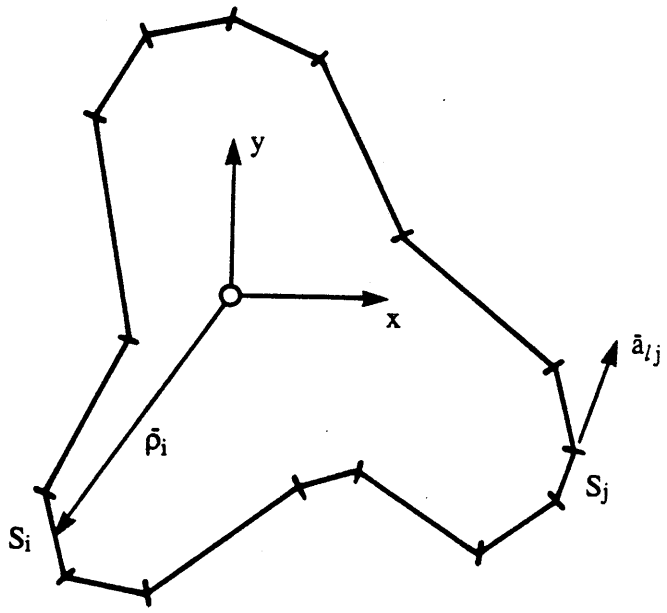

Fig. 3. Segmentation of the patch.

$$+\frac{i}{2\pi\omega\mu_0\Delta_i}\oint_P dl'\,\frac{\partial V}{\partial l'}\,G_d(l,l')\Big|_{\bar{\rho}=\bar{\rho}_i+\bar{a}_{li}\Delta_i/2}^{\bar{\rho}=\bar{\rho}_i-\bar{a}_{li}\Delta_i/2}$$

$$-\frac{i\omega\epsilon_0}{\pi}\,V(l_i)\,F(\epsilon_r)\;-\;\frac{i}{\pi\omega\mu_0}\,\frac{\partial^2 V}{\partial l^2}\Big|_{l=l_i}\,F(\frac{1}{\mu_r}) \qquad (47)$$

This GEBC allows the efficient and accurate analysis of various patch structures of arbitrary shapes. Some applications will be presented in a forthcoming report.

6. PERTURBATION APPROACH

It is well known that the cavity model [9]-[11] provides an efficient way of analyzing microstrip patch antennas and resonators. Closed form results can be obtained for simple patch shapes such as rectangles, circles and ellipses. Opinions differ, however, on what kind of boundary condition should be imposed at the edge of the patch. This inability to find an accurate boundary condition has originated mainly from the complexity of the field behavior close to the edge. Our generalized boundary condition is well suited for developing

a perturbation approach. The unperturbed problem will be that of a closed cavity under the patch, with perfectly electrically conducting top and bottom walls and perfectly magnetically conducting side walls. This representation is often called an "ideal" cavity model. The perturbed situation will correspond to the actual patch, with dynamical edge effects, radiation and coupling between edges. We will consider here unloaded patch resonators only.

Following the normalization (22), we can define a voltage from the z-directed component of the TEM electric field:

$$V = -E_z^{TEM}\, d \tag{48}$$

The true voltage satisfies the source-free wave equation:

$$(\nabla_t^2 + k^2)V = 0 \tag{49}$$

where $\nabla_t = \hat{a}_x\, \partial/\partial_x + \hat{a}_y\, \partial/\partial_y$. Faraday's equation applied at the edge of the patch, for $0 < z < d$, yields directly

$$\frac{\partial V}{\partial n}\Big|_{on\ P} = -i\omega\mu_0\mu_r\, d\, H_t^{TEM}\Big|_{on\ P} \tag{50}$$

The "ideal" cavity model voltage for the same patch satisfies the equation:

$$(\nabla_t^2 + \tilde{k}^2)\tilde{V} = 0 \tag{51}$$

with the boundary condition

$$\frac{\partial \tilde{V}}{\partial n}\Big|_{on\ P} = 0$$

where we have indicated with a tilde all variables pertaining to the "ideal" cavity model. Recall Green's theorem [17]:

$$\int_{S_C} ds\, (V\nabla_t^2\tilde{V} - \tilde{V}\nabla_t^2 V) = \oint_P dl\, \left(V\frac{\partial\tilde{V}}{\partial n} - \tilde{V}\frac{\partial V}{\partial n}\right) \tag{52}$$

Substituting the wave equations (49) and (51) into (52), and using a standard procedure, we find the correction for eigenvalues:

$$k^2 - \tilde{k}^2 = \frac{i\omega\mu_0\mu_r\, d \oint_P dl\ \tilde{V}(l)\, H_t^{TEM}(l)}{\int_{S_C} ds\ V\tilde{V}} \tag{53}$$

The numerator can be readily evaluated if we recall our generalized boundary condition (43) with $\Lambda(l) = \tilde{V}(l)$. In what is the key feature of a perturbation procedure [18], we then approximate the edge voltage $V(l)$ by its cavity-model counterpart $\tilde{V}(l)$. Then,

$$k^2 - \tilde{k}^2 \simeq \frac{i\omega\mu_0\mu_r\, d\,(N_1 + N_2)}{\int\limits_{S_C} ds\ \tilde{V}^2} \tag{54}$$

with

$$N_1 = \frac{i\omega\epsilon_0}{2\pi} \oint\limits_P dl \oint\limits_P dl'\ [\bar{a}_{l'} \cdot \bar{a}_l]\ \tilde{V}(l)\,\tilde{V}(l')\,G_d(l,l') - \frac{i\omega\epsilon_0}{\pi}\ F(\epsilon_r) \oint\limits_P dl\ \tilde{V}^2 \tag{55}$$

$$N_2 = \frac{-i}{2\pi\omega\mu_0} \oint\limits_P dl \oint\limits_P dl'\ \frac{\partial\tilde{V}}{\partial l}\ \frac{\partial\tilde{V}}{\partial l'}\ G_d(l,l') + \frac{i}{\pi\omega\mu_0}\ F(\frac{1}{\mu_r}) \oint\limits_P dl\ (\frac{\partial\tilde{V}}{\partial l})^2 \tag{56}$$

where we have integrated by parts to obtain the term N_2.

Once the perturbed eigenvalues k are computed, we can easily find the corresponding unloaded quality factor Q [19]:

$$Q = \frac{\mathrm{Re}(k)}{2\,\mathrm{Im}(k)} \tag{57}$$

7. THEORY OF THE RECTANGULAR PATCH ANTENNA

The rectangular microstrip antenna has received more attention than all other shapes taken together. The simplicity of the geometry has led to many specialized techniques. Furthermore, even the most general numerical techniques usually work better on rectangular shapes. Finally, because of the large amount of experimental data available in the literature, the rectangular patch has become a benchmark for comparisons.

First attempts to analyze the rectangular patch antenna were made by Munson [6] and Derneryd [7], [20] in the mid-seventies. They used an analogy with a section of transmission line terminated by lumped impedances. This method became known as the transmission-line model and was later refined by Dubost [21], Lier [22] and Pues and Van de Capelle [8]. Approximate formulas for the resonant frequency based on the same approach have been given by Sengupta [23].

At the same time, microstrip antennas were also looked at as resonators. Wolff and Knoppik [24] introduced equivalent dimensions and dielectric constants to simulate the effects of the fringing field. Lo et al. [9], [25], Richards et al. [10] and Derneryd and Lind [26] improved and completed what has been called the cavity model. Simultaneously, Carver [27] and Carver and Mink [11] have presented a technique based on modal expansion and lumped equivalent wall admittances.

Using a very different point of view, Chang [28] and Kuester et al. [29] have considered the rectangular patch using a transverse resonance model, where TEM waves bounce off the edges of the patch. Analytical results for the resonant frequency and the Q-factor, valid for electrically thin substrates, are given in [29].

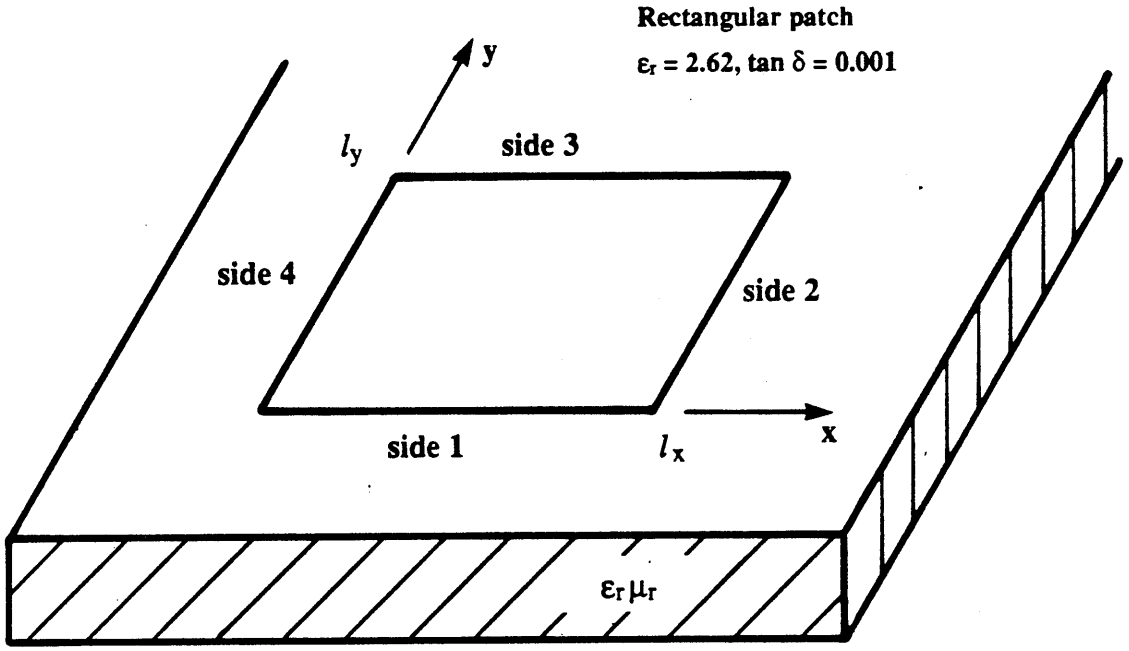

Fig. 4. Rectangular microstrip patch.

Lastly, many different numerical approaches have been proposed. In 1973 already, Silvester introduced a finite element analysis [30]. Two years later, Akhtarzad and Johns [31] presented a transmission-line matrix (TLM) approach. However, these two techniques have difficulty including radiation and surface wave effects. Later, Itoh and Menzel [1] have presented a dynamic full-wave analysis based on an integral transform of the wave equation. In what appears the most accurate analysis available, several authors have presented models based on direct solution of the integral equation for the patch current. Bailey and Deshpande [2], Newman and Tulyathan [32], Mosig and Gardiol [4], [5] and Pozar [3] have all given results for the rectangular patch. Recently, Shimin [33] has given approximate formulas based on [2]. In all cases, numerical methods appear handicapped by lengthy computing times.

In this section, we will compute the resonant frequency and the quality factor of a rectangular microstrip patch, based on the expressions (54) and (57). The results can be expressed in a simple form for the modes TM_{10} and TM_{01}.

Consider the geometry of the rectangular patch shown in Fig. 4. The solution of the "ideal" cavity model, with magnetic walls at x = 0, l_x and y = 0, l_y, is easily obtained by separation of variables in the two dimensional wave equation (51). For the sake of clarity, we will limit ourselves to the dominant mode TM_{10}. Along the edges of the patch:

$$\tilde{V}(x=0) = A_{10} \qquad 0 \le y \le l_y \tag{58a}$$

$$\tilde{V}(x=l_x) = -A_{10} \qquad 0 \le y \le l_y \tag{58b}$$

$$\tilde{V}(y=0) = A_{10}\cos(\frac{\pi x}{l_x}) \qquad 0 \le x \le l_x \tag{58c}$$

$$\tilde{V}(y=l_y) = A_{10}\cos(\frac{\pi x}{l_x}) \qquad 0 \le x \le l_x \tag{58d}$$

where A_{10} is the mode amplitude constant for the mode TM_{10}. Recall the correction for the eigenvalues given by equation (54):

$$k^2 - \tilde{k}^2 \simeq \frac{i\omega\mu_0\mu_r\, d\,(N_1 + N_2)}{\int_{S_C} ds\ \tilde{V}^2}$$

with

$$N_1 = \frac{i\omega\epsilon_0}{2\pi} \oint_P dl \oint_P dl'\ [\bar{a}_{l'} \cdot \bar{a}_l]\ \tilde{V}(l)\,\tilde{V}(l')\,G_d(l,l') - \frac{i\omega\epsilon_0}{\pi}\ F(\epsilon_r) \oint_P dl\ \tilde{V}^2$$

$$N_2 = \frac{-i}{2\pi\omega\mu_0} \oint_P dl \oint_P dl'\ \frac{\partial\tilde{V}}{\partial l}\ \frac{\partial\tilde{V}}{\partial l'}\ G_d(l,l') + \frac{i}{\pi\omega\mu_0}\ F(\frac{1}{\mu_r}) \oint_P dl\ (\frac{\partial\tilde{V}}{\partial l})^2$$

It is convenient to number the sides of the rectangular patch as indicated in Fig. 4, to obtain

$$N_1 = \frac{i\omega\epsilon_0}{2\pi} \sum_{i=1}^{4}\sum_{j=1}^{4} I_{ij} - \frac{i\omega\epsilon_0}{\pi}\ F(\epsilon_r) \oint_P dl\ \tilde{V}^2 \tag{59}$$

where the coupling integrals I_{ij} are given by

$$I_{ij} = \int_{\text{side } i} dl \int_{\text{side } j} dl'\ \tilde{V}(l)\,\tilde{V}(l')\,[\bar{a}_{li} \cdot \bar{a}_{lj}]\,G_d(l,l') \tag{60}$$

Because of the symmetry of the geometry and the scalar product $[\bar{a}_{li} \cdot \bar{a}_{lj}]$, we are left with four terms only. Note also that, without loss of generality, we can set the arbitrary mode amplitude constant A_{10} to unity. Therefore,

$$N_1 = \frac{i\omega\epsilon_0}{\pi}\left[I_{11} + I_{13} + I_{22} + I_{24} - F(\epsilon_r)(l_x + 2l_y)\right] \tag{61}$$

where

$$I_{11} = \int_0^{l_x} dx \int_0^{l_x} dx'\ \cos\tilde{k}x\cos\tilde{k}x'\ \frac{e^{-ik_0((x-x')^2+d^2)^{1/2}}}{((x-x')^2+d^2)^{1/2}} \tag{62a}$$

$$I_{13} = -\int_0^{l_x} dx \int_0^{l_x} dx' \cos\tilde{k}x \cos\tilde{k}x' \frac{e^{-ik_0((x-x')^2 + l_y^2 + d^2)^{1/2}}}{((x-x')^2 + l_y^2 + d^2)^{1/2}} \tag{62b}$$

$$I_{22} = \int_0^{l_y} dy \int_0^{l_y} dy' \frac{e^{-ik_0((y-y')^2 + d^2)^{1/2}}}{((y-y')^2 + d^2)^{1/2}} \tag{62c}$$

$$I_{24} = \int_0^{l_y} dy \int_0^{l_y} dy' \frac{e^{-ik_0((y-y')^2 + l_x^2 + d^2)^{1/2}}}{((y-y')^2 + l_x^2 + d^2)^{1/2}} \tag{62d}$$

where $\tilde{k} = \pi/l_x$ is the dominant mode, unperturbed, wavenumber. The integral I_{11} can be approximated in closed form as shown in Appendix E:

$$I_{11} = l_x\, Ci(\pi) - \frac{Si(\pi)}{\tilde{k}} - \frac{\pi}{\tilde{k}}(\gamma + \ln(d/2)) - \frac{\pi \ln(\tilde{k}^2 - k_0^2)}{2\tilde{k}}$$

$$+ i\left[\frac{1}{\tilde{k} + k_0} - \frac{\tilde{k} + k_0\, e^{-ik_0 l_x}}{\tilde{k}^2 - k_0^2} + \frac{1}{2\tilde{k}} \ln\left(\frac{\tilde{k} + k_0}{\tilde{k} - k_0}\right)\right] - \frac{(i+\pi)}{2\tilde{k}} E_1(ik_0 l_x - i\pi)$$

$$+ \frac{(i-\pi)}{2\tilde{k}} E_1(ik_0 l_x + i\pi) + \frac{Si(\pi) - \pi/2 - \pi\, Ci(\pi)}{\tilde{k}} \tag{63}$$

where the cosine integral Ci, sine integral Si and exponential integral E_1 functions are defined in Appendixes E and F. This approximation, valid for small $k_0 d$, may fail to give accurate results for electrically thick substrates. A better approximation could presumably be derived using the Mellin Transform approach [29]. Another, more practical, approach is to seek a numerically efficient expression such as the one proposed in Appendix G:

$$I_{11} = \int_0^{l_x} dp \frac{e^{-ik_0(p^2+d^2)^{1/2}}\left[(l_x - p)\cos\tilde{k}p - \frac{\sin\tilde{k}p}{\tilde{k}}\right] - l_x}{(p^2 + d^2)^{1/2}} + l_x \sinh^{-1}(l_x/d) \tag{64}$$

Comparisons between the expressions (63) and (64) show that the relative error in (63) is probably of order $\tilde{k}d$ (Fig. 5). The approximation (63) has however proved to be satisfactory for all cases tested. The terms I_{13}, I_{22} and I_{24} can all be expressed in a numerically efficient form (Appendix G):

$$I_{13} = -\int_0^{l_x} dp \frac{e^{-ik_0(p^2 + l_y^2 + d^2)^{1/2}}\left[(l_x - p)\cos\tilde{k}p - \frac{\sin\tilde{k}p}{\tilde{k}}\right]}{(p^2 + l_y^2 + d^2)^{1/2}} \tag{65}$$

$$I_{22} = 2\int_0^{l_y} dp \frac{(l_y - p)\, e^{-ik_0(p^2+d^2)^{1/2}} - l_y}{(p^2 + d^2)^{1/2}} + 2\, l_y \sinh^{-1}(l_y/d) \tag{66}$$

$$I_{24} = 2\int_0^{l_y} dp\, (l_y - p) \frac{e^{-ik_0(p^2 + l_x^2 + d^2)^{1/2}}}{(p^2 + l_x^2 + d^2)^{1/2}} \tag{67}$$

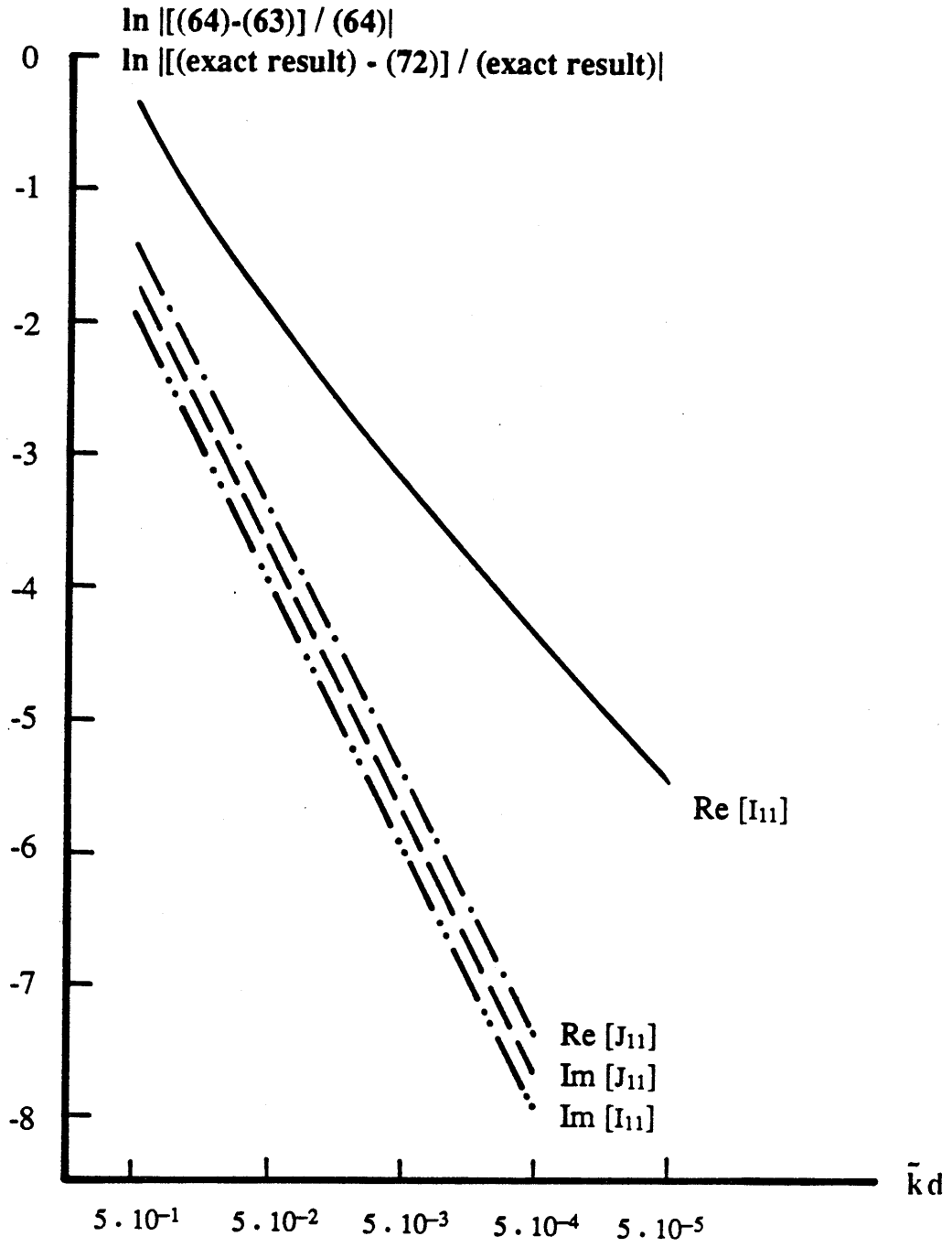

Fig. 5. Relative error on terms I_{11} and J_{11}.

The term N_2 can be written

$$N_2 = \frac{-i}{2\pi\omega\mu_0} \sum_{i=1}^{4} \sum_{j=1}^{4} J_{ij} + \frac{i}{\pi\omega\mu_0} F(\frac{1}{\mu_r}) \oint_P dl \left(\frac{\partial \tilde{V}}{\partial l}\right)^2 \tag{68}$$

where the coupling integrals are given by

$$J_{ij} = \int_{side\ i} dl \int_{side\ j} dl' \frac{\partial \tilde{V}}{\partial l} \frac{\partial \tilde{V}}{\partial l'} G_d(l,l') \tag{69}$$

Because the derivative of the edge voltage, $\partial \tilde{V}/\partial l$, vanishes along the sides 2 and 4, and because of the symmetry of the geometry, (68) reduces to

$$N_2 = \frac{-i}{\pi\omega\mu_0} \left[J_{11} + J_{13} - F(\frac{1}{\mu_r}) \frac{\pi^2}{l_x} \right] \tag{70}$$

where

$$J_{11} = \tilde{k}^2 \int_0^{l_x} dx \int_0^{l_x} dx' \sin \tilde{k}x \sin \tilde{k}x' \frac{e^{-ik_0\left((x-x')^2 + d^2\right)^{1/2}}}{\left((x-x')^2 + d^2\right)^{1/2}} \tag{71a}$$

$$J_{13} = -\tilde{k}^2 \int_0^{l_x} dx \int_0^{l_x} dx' \sin \tilde{k}x \sin \tilde{k}x' \frac{e^{-ik_0\left((x-x')^2 + l_y^2 + d^2\right)^{1/2}}}{\left((x-x')^2 + l_y^2 + d^2\right)^{1/2}} \tag{71b}$$

A closed form expression for J_{11} can be obtained along the same lines as for the term I_{11}:

$$J_{11} = i\tilde{k} \left(\frac{-\pi^2 H}{2} - \ln(\tilde{k} + k_0) + \frac{\tilde{k}}{\tilde{k} + k_0} - \left(\frac{1 + i\pi}{2}\right) \left[i\pi - \ln(\tilde{k}^2 - k_0^2) \right] \right.$$

$$\left. - \tilde{k} \left(\frac{\tilde{k} + k_0 e^{-ik_0 l_x}}{\tilde{k}^2 - k_0^2} \right) + \frac{1}{2} \left[(1 + i\pi) E_1(ik_0 l_x - \pi) - (1 - i\pi) E_1(ik_0 l_x + i\pi) \right] \right) \tag{72}$$

Comparisons between the approximation (72) and the exact result shows that the relative error is of order $(\tilde{k}d)^2$ (Fig. 5). The expression (72) is thus valid in all cases within the frame of our theoretical development. Following Appendix G, J_{13} can be written in a form that suits numerical integration:

$$J_{13} = -\tilde{k}^2 \left[\int_0^{l_x} dp \frac{e^{-ik_0\left(p^2 + l_y^2 + d^2\right)^{1/2}} \left[(l_x - p) \cos \tilde{k}p + \frac{\sin \tilde{k}p}{\tilde{k}} \right]}{(p^2 + l_y^2 + d^2)^{1/2}} \right] \tag{73}$$

Since,

$$\int_{S_C} ds\ \tilde{V}^2 = \frac{l_x l_y}{2} \tag{74}$$

the eigenvalue shift for the TM_{10} is given by equation (54):

$$k_{10}^2 - \tilde{k}_{10}^2 = \frac{2i\omega\mu_0\mu_r d}{l_x l_y}\left[\frac{i\omega\epsilon_0}{\pi}\left(I_{11} + I_{13} + I_{22} + I_{24} - F(\epsilon_r)(l_x + 2l_y)\right)\right.$$

$$\left.\frac{-i}{\pi\omega\mu_0}\left(J_{11} + J_{13} - F(\frac{1}{\mu_r})\frac{\pi^2}{l_x}\right)\right] \tag{75}$$

Interchanging l_x and l_y, the above result gives directly the correction for the eigenvalue of the TM_{01} mode.

8. RESULTS FOR THE RECTANGULAR PATCH

In order to assess the value of our theory, it is essential to check it against experimental results and other theoretical approaches. By choosing published experimental data, we have minimized the risk of biased comparisons. Among the relatively large quantity of publications available, we have selected the measurements of Y.T. Lo and his group in Illinois because of their reliability and accessibility.

In [9], Y.T. Lo et al. present measured results for the resonant frequencies and Q-factors for different rectangular patches. An interesting feature is that the length of the non radiating edge is kept constant. This provides a clear visualization of effects impossible to see with an "ideal" cavity model.

On the theoretical side, we have compared our approach with Carver's modal expansion model [27] and Kuester et al.'s wide patch analytical formulation [29]. To help the reader, we have collected the detailed calculations for all three theoretical models in Appendix H.

Fig. 6 shows the results for the resonant frequencies. Care must be exercised in interpreting the results. The theoretical curves are indeed very sensitive to minute changes in the dielectric constant of the substrate. It is thus not surprising that we do not see an overlap of experimental and theoretical curves. More meaningful is the relative position of the theoretical curves and the shape correlation of the curves between experimental and theoretical results.

Note the complete failure of the "ideal" cavity model to take into account variations in the length of the radiating edge (l_y). Remark also the limitations of Carver's theory for wide patches. Finally, observe the good behavior of the present theory, which predicts the shape of the curve almost exactly without using any equivalent parameters such as edge extension or effective dielectric constant.

Fig. 7 shows the results for the Q-factor. Note the excellent agreement between our theory and the experimental results.

Although numerical integrations are needed in the present model, the required computational effort is very small. Typically, ten points in a Gaussian quadrature are more than enough.

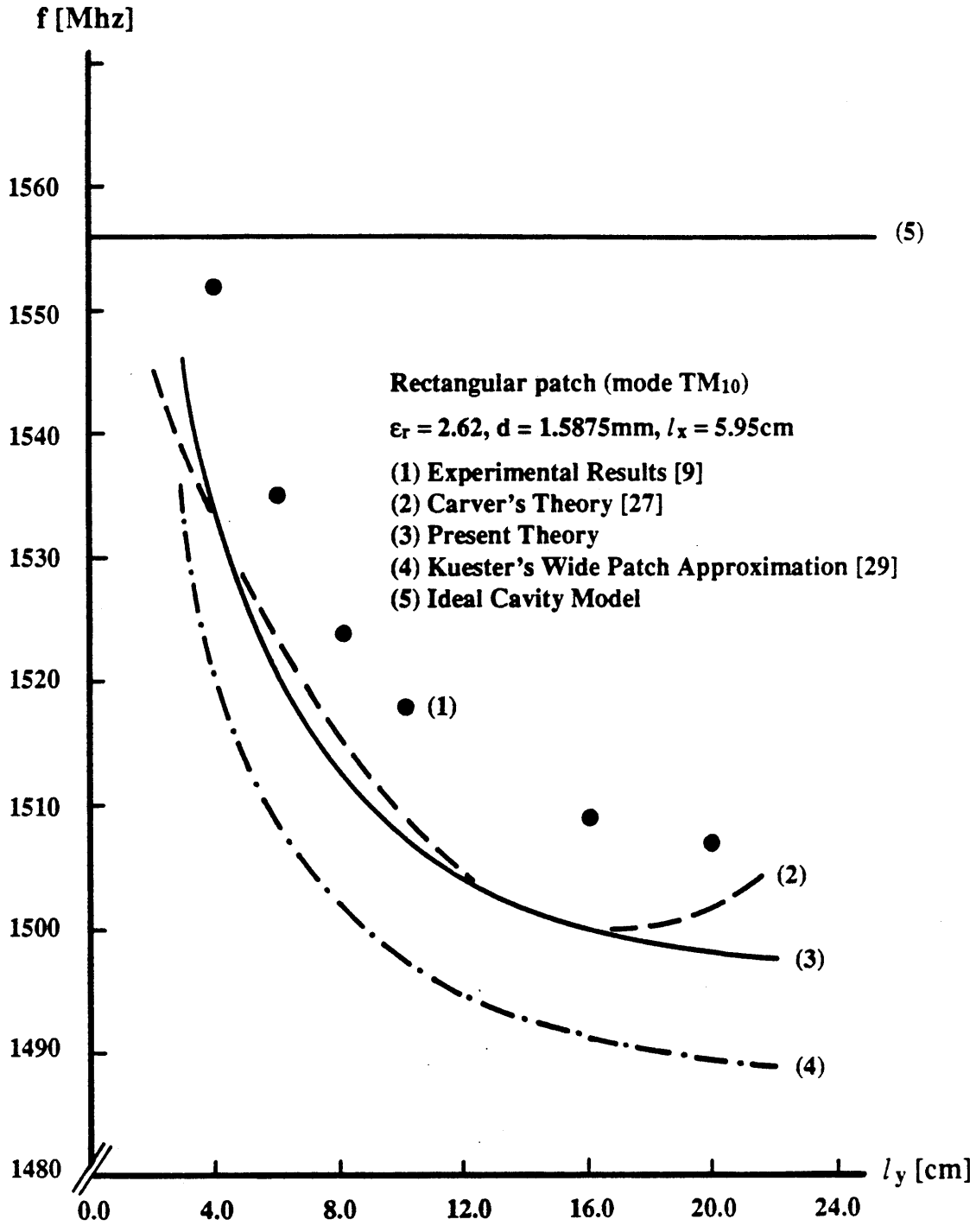

Fig. 6. Resonant frequency. (Rectangular Patch).

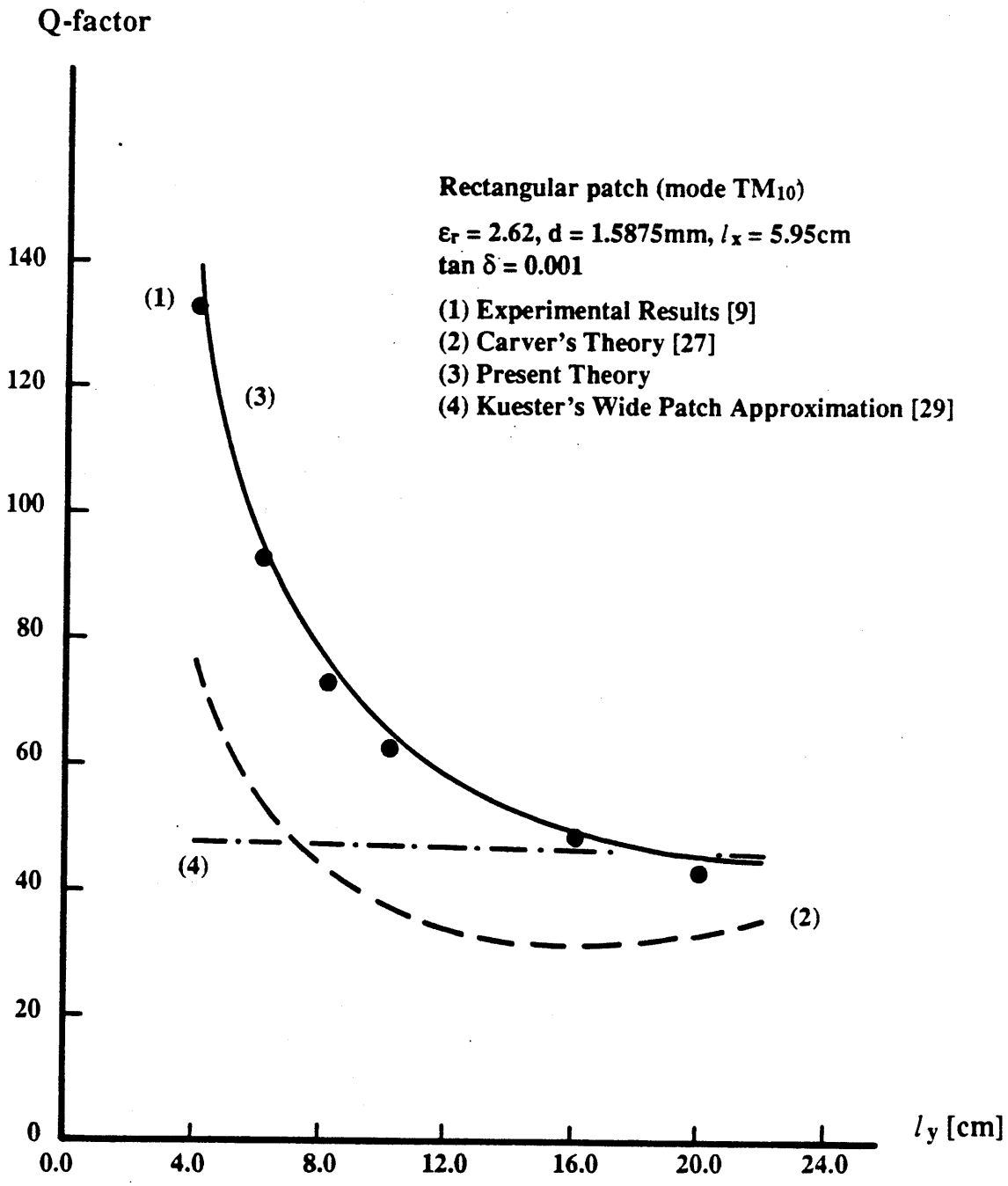

Fig. 7. Q-factor. (Rectangular patch).

9. THEORY OF THE CIRCULAR PATCH ANTENNA

Because of the axial symmetry, the circular microstrip patch antenna has called for specialized analytical techniques. At the same time, people have adapted "classical" approaches, such as the cavity model, to this geometry.

Watkins [34] obtained first the resonant frequencies for a circular patch using an "ideal" cavity model. Next, attention was focused on quasi-static approaches to give corrections for the "fringing" field. A detailed account of earlier work to solve the static circular capacitor has been given by Kuester [35]. Numerical computations for the same problem have been presented by Itoh and Mittra [36]. Borkar and Yang [37], Coen and Gladwell [38] and Mosig [39] improved later the numerical formulation. Wolff and Knoppik [24] and Shen et al. [40] have given formulas for the resonant frequency based on this quasi-static approach.

Cavity model results have been presented by many authors. Long et al. [41], [42] and Derneryd [43] were the first to give such an analysis. Later, Carver [27], Richards et al. [10] and Yano and Ishimaru [44] refined the model. More recently, Davidovitz and Lo [45] have adapted the cavity model to thicker substrates.

Chew and Kong [46]-[49] have studied the resonance with various techniques. In particular, they have given asymptotic formulas valid for thin substrates [48], and have solved dual integral equations using a Hankel transform approach [49].

Araki and Itoh [50] have used a full wave analysis with spectral domain basis functions, and Wood [51] has employed a similar technique with spatial domain basis functions. Quite recently, Dubost and Beauquet [52] adapted a transmission-line type of approach to the circular patch.

Few numerical solutions based on the integral equation for patch current have been proposed, probably because of the difficulties in discretizing the circular surface in elementary cells. Agrawal and Bailey [53] considered the circular patch in their early approach with a homogeneous Green function. Butler [12] has presented a technique based on an aperture integral equation. Recently, Bailey and Deshpande [54] have looked specifically at the circular patch with a moment method solution.

In this section, we will compute the resonant frequency and the Q-factor of the dominant mode TM_{11} of the circular patch, based on expressions (54) and (57). Consider the geometry of the circular microstrip patch antenna shown in Fig. 8. The solution of the "ideal" cavity model is obtained by solving the wave equation (51) together with a Neumann boundary condition at the edge of the patch [55]. If R denotes the radius of the patch, the unperturbed wavenumber $\tilde{k}$ is solution of the eigenvalue equation:

$$J_n'(\tilde{k}R) = 0 \tag{76}$$

where J_n is the Bessel function of order n and the prime indicates the derivative with respect to the argument. Recalling a conventional notation [56],

$$\tilde{k}R = j'_{n,m} \tag{77}$$

where $j'_{n,m}$ is the m^{th} positive zero of J_n'. For the dominant (non static) mode TM_{11},

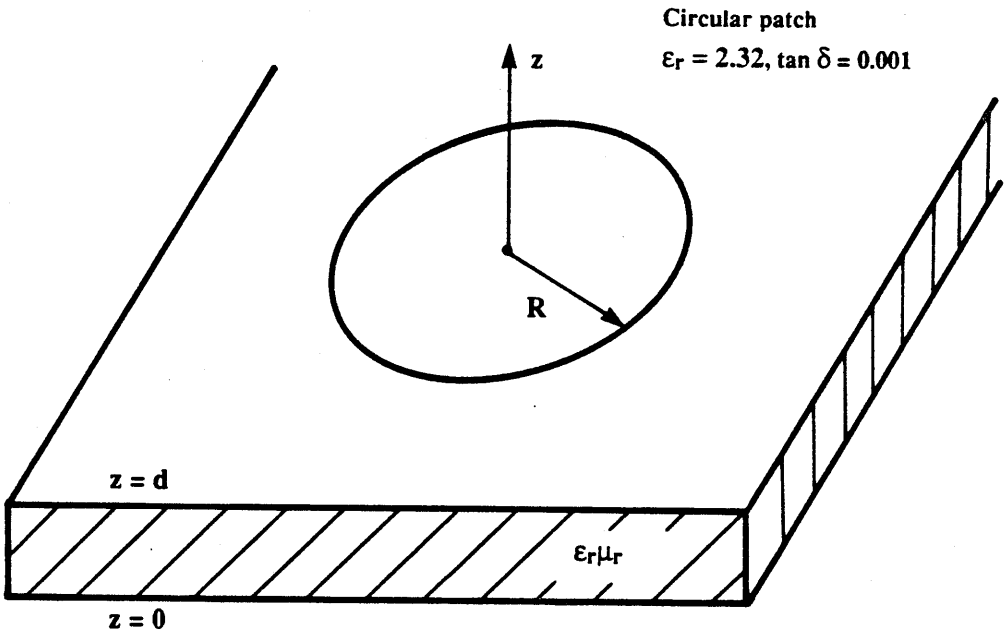

Fig. 8. Circular microstrip patch.

$$\tilde{k}_{11} = \frac{j'_{1,1}}{R} \tag{78}$$

with $j'_{1,1} = 1.8411837\ldots$. The edge voltage $\tilde{V}$ and its edge derivative $\partial\tilde{V}/\partial l$ are given by

$$\tilde{V} = A_{11} d\, \mathrm{J}_1\left(\frac{j'_{1,1}\rho}{R}\right)\cos\phi \tag{79}$$

$$\frac{\partial\tilde{V}}{\partial l} = -\frac{A_{11} d}{R}\, \mathrm{J}_1\left(\frac{j'_{1,1}\rho}{R}\right)\sin\phi \tag{80}$$

where A_{11} is an arbitrary mode amplitude factor. Without loss of generality, we can set this amplitude coefficient to unity. The correction for the eigenvalue is given by equation (54):

$$k_{11}^2 - \tilde{k}_{11}^2 = \frac{i\omega\mu_0\mu_r d\,(N_1 + N_2)}{I_S} \tag{81}$$

where

$$I_S = \int_{S_C} ds\ \tilde{V}^2 \tag{82}$$

while the terms N_1 and N_2 are given by (55) and (56). For the circular geometry,

$$N_1 = \frac{i\omega\epsilon_0}{2\pi}\ I_C - \frac{i\omega\epsilon_0}{\pi}\ F(\epsilon_r)\ \oint_P dl'\ \tilde{V}^2(l') \tag{83}$$

where the coupling integral I_C is given by

$$I_C = \oint_P dl \oint_P dl' \left[\bar{a}_l \cdot \bar{a}_{l'}\right]\ \tilde{V}(l)\ \tilde{V}(l')\ G_d(l,l') \tag{84}$$

Similarly,

$$N_2 = \frac{-i}{2\pi\omega\mu_0}\ J_C + \frac{i}{\pi\omega\mu_0}\ F(\frac{1}{\mu_r}) \oint_P dl'\ \left(\frac{\partial\tilde{V}}{\partial l'}\right)^2 \tag{85}$$

with the coupling integral

$$J_C = \oint_P dl \oint_P dl'\ \frac{\partial\tilde{V}}{\partial l}\ \frac{\partial\tilde{V}}{\partial l'}\ G_d(l,l') \tag{86}$$

The three integrals I_C, J_C and I_S are computed in Appendix I:

$$I_C = 2\pi\left[dR\ \mathrm{J}_1(j'_{1,1})\right]^2\left[\ \frac{2\,\mathbf{K}\left(\frac{4R^2}{4R^2+d^2}\right)}{(4R^2+d^2)^{1/2}} + \int_0^{\pi} d\alpha\ \frac{\cos^2\alpha\ e^{-ik_0\left(4R^2\sin^2(\alpha/2)+d^2\right)^{1/2}} - 1}{\left(4R^2\sin^2(\alpha/2)+d^2\right)^{1/2}}\ \right] \tag{87}$$

where $\mathbf{K}$ is the complete elliptic integral of the first kind, whose argument (following Milne-Thomson) is taken as the modulus squared [57];

$$J_C = 2\pi d^2\,\mathrm{J}_1^2(j'_{1,1})\left[\ \frac{2\mathbf{K}\left(\frac{4R^2}{4R^2+d^2}\right)}{(4R^2+d^2)^{1/2}} + \int_0^{\pi} d\alpha\ \frac{\cos\alpha\ e^{-ik_0\left(4R^2\sin^2(\alpha/2)+d^2\right)^{1/2}} - 1}{\left(4R^2\sin^2(\alpha/2)+d^2\right)^{1/2}}\ \right] \tag{88}$$

and

$$I_S = \frac{\pi d^2R^2}{2}\left(1 - \frac{1}{j'^2_{1,1}}\right)\mathrm{J}_1^2(j'_{1,1}) \tag{89}$$

The remaining integrals in equations (83) and (85) are straightforward

$$\oint_P dl'\ \tilde{V}^2(l') = \pi d^2 R\ \mathrm{J}_1^2(j'_{1,1}) \tag{90}$$

$$\oint_P dl'\ \left(\frac{\partial\tilde{V}}{\partial l'}\right)^2 = \frac{\pi d^2}{R}\ \mathrm{J}_1^2(j'_{1,1}) \tag{91}$$

We then have all the terms we need to compute directly the eigenvalue shift from equation (81).

10. RESULTS FOR THE CIRCULAR PATCH ANTENNA

We have compared our theoretical results for the dominant mode TM_{11} with experimental data and Carver's modal expansion theory [27]. Unlike the rectangular patch, complete data for the resonant frequencies and Q-factors are not widely available. Long et al. [41], [42] and Wood [51] have however published fairly detailed results. We have chosen the latter for direct comparisons against our theory.

We again have used Carver's modal expansion model [27] as theoretical comparison. His results, based on some empirical considerations, have usually proved to be in good agreement with measurements. To help the reader, we have collected the detailed calculations for the two theoretical models in Appendix J.

Fig. 9 shows the resonant frequency of a circular patch versus the ratio of the radius of the patch to the height of the substrate. Fig. 10 gives the Q-factor for the same patch. Note that for small thicknesses d, the Q-factor, as expected, grows substantially. As a consequence, we cannot neglect conduction losses any more. James et al. [58] give a simple way to take care of this effect efficiently. Through an equivalent conductance loss Q-factor, they are able to match experimental results for high Q's. The same technique can easily be applied to our results.

11. CONCLUSION

A new approach has been applied here to the analysis of arbitrarily shaped microstrip resonators and antennas. The model yields a generalized boundary condition at the edge of a microstrip patch. Unlike previous theories, this GEBC has contributions from the whole contour of the structure taking care of mutual coupling effects.

Based on this GEBC, we can analyze arbitrarily patches after a segmentation of the contour. Successful results will be presented in a forthcoming report and a soon to be published technical paper [59].

Directly from this GEBC, we have developed a perturbation approach for computing resonant frequencies and Q-factors for geometries where the wave equation has a closed-form solution. Simple expressions have been given for the dominant modes of the rectangular and circular patches. Theoretical results agree well with experimental results. In particular, computed Q-factors are always in much better agreement with experimental data than the modal expansion model.

The absence of artificial parameters such as edge extensions, the accuracy of the results and the relative simplicity of the computations make the approach described in this report very suitable for the analysis of microstrip antennas and resonators in a CAD context.

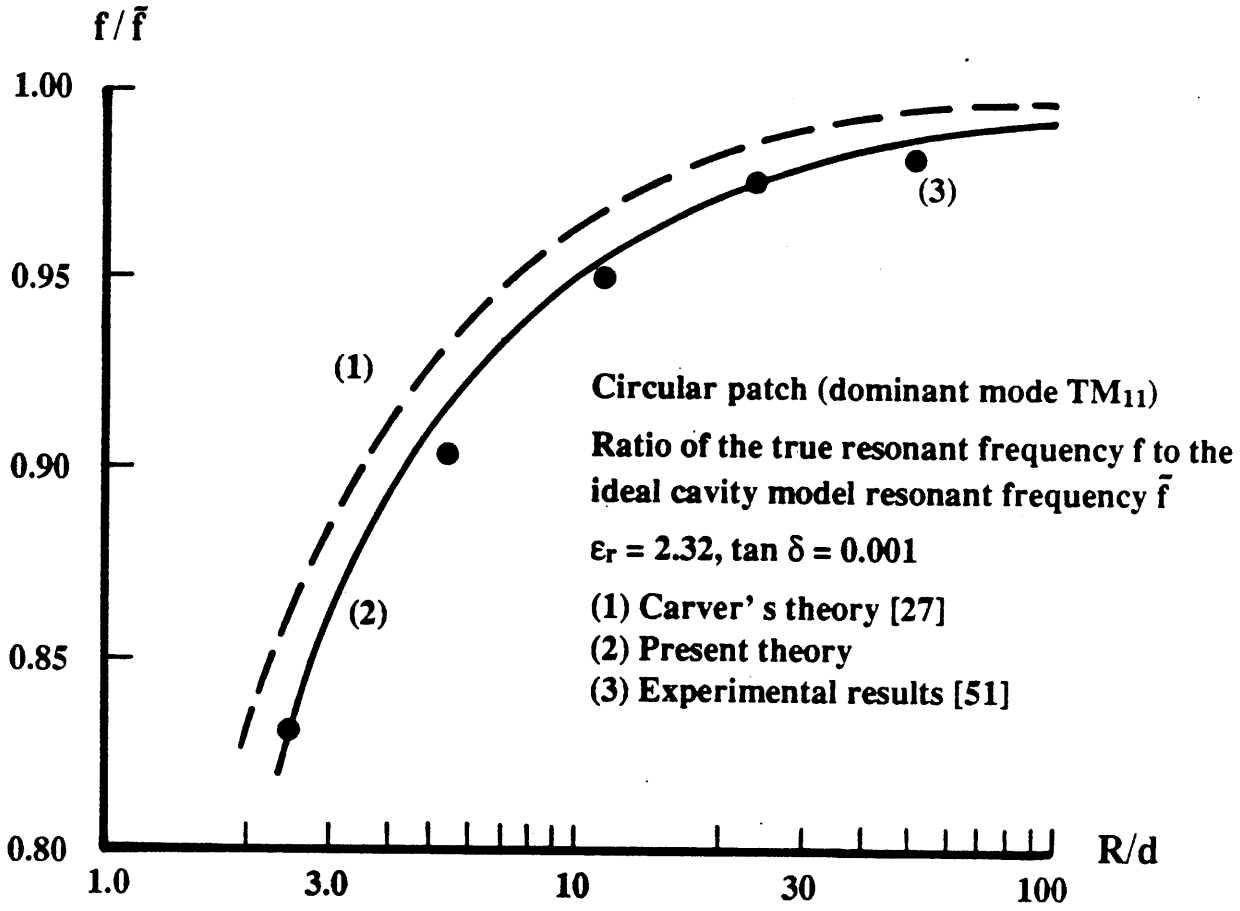

Fig. 9. Resonant frequency. (Circular patch).

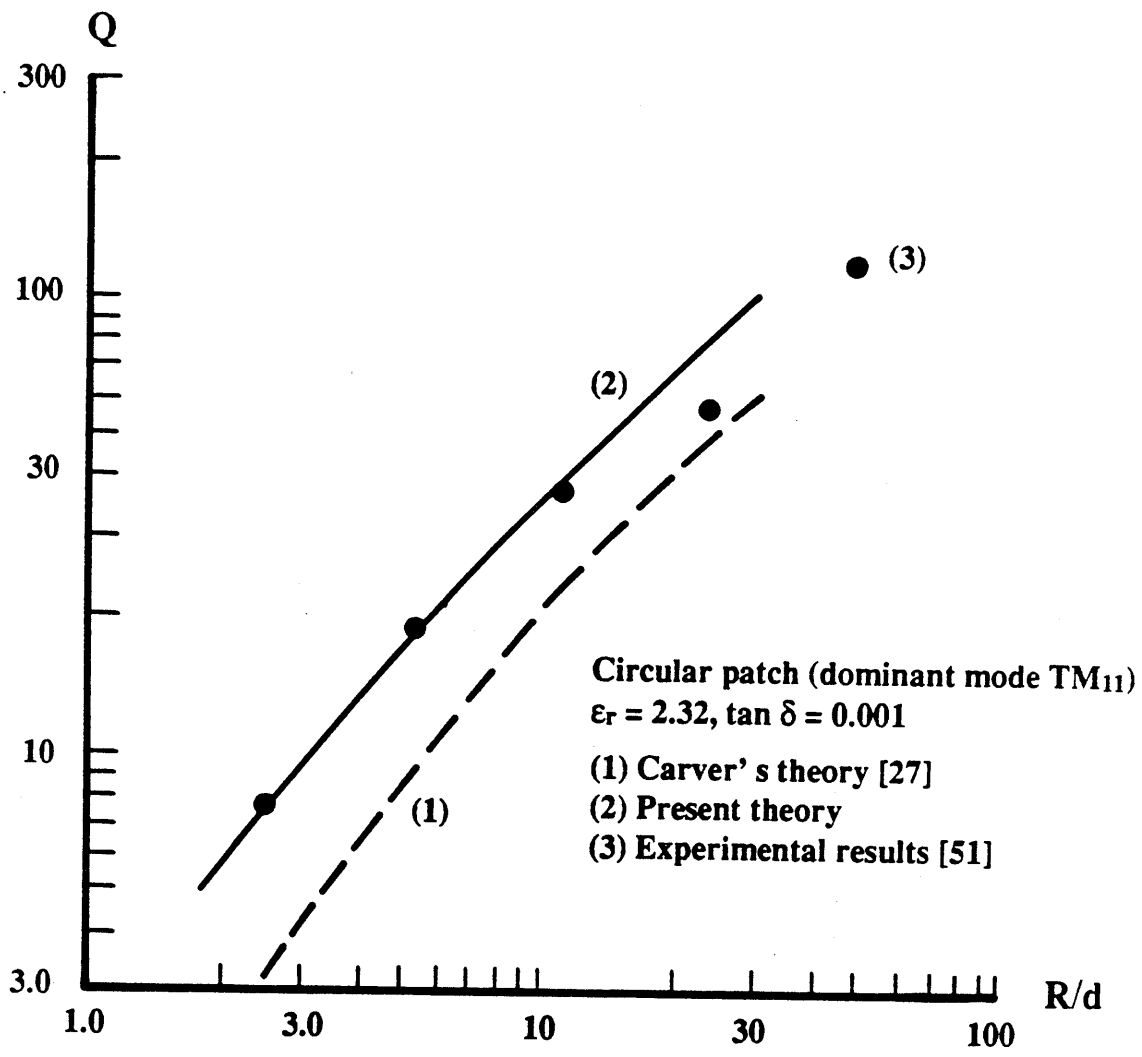

Fig. 10. Q-factor. (Circular patch).

REFERENCES

[1] T. Itoh and W. Menzel, "A full-wave analysis method for open microstrip structures", *IEEE Trans. Antennas Propagat.*, vol. 29, pp. 63-68, Jan. 1981.

[2] M.C. Bailey and M.D. Deshpande, "Integral equation formulation of microstrip antennas", *IEEE Trans. Antennas Propagat.*, vol. 30, pp. 651-656, July 1982.

[3] D.M. Pozar, "Input impedance and mutual coupling of rectangular microstrip antennas," *IEEE Trans. Antennas Propagat.*, vol. 30, pp. 1191-1196, Nov. 1982.

[4] J.R. Mosig and F.E. Gardiol, "Analytical and numerical techniques in the Green's function treatment of microstrip antennas and scatterers," *IEE Proc., pt. H,* vol. 130, pp. 175-182, Mar. 1983.

[5] J.R. Mosig and F.E. Gardiol, "General integral equation formulation for microstrip antennas and scatterers," *IEE Proc., pt. H,* vol. 132, pp. 424-432, Dec. 1985.

[6] R.E. Munson, "Conformal microstrip antennas and microstrip phased arrays," *IEEE Trans. Antennas Propagat.*, vol. 22, pp. 74-78, Jan. 1974.

[7] A.G. Derneryd, "Linearly polarized microstrip antennas," *IEEE Trans. Antennas Propagat.*, vol. 24, pp. 846-851, Nov. 1976.

[8] H. Pues and A. Van de Capelle, "Accurate transmission-line model for the rectangular microstrip antenna," *IEE Proc., pt. H,* vol. 131, pp. 334-340, Dec. 1984.

[9] Y.T. Lo, D. Solomon, and W.F. Richards, "Theory and experiment on microstrip antennas," *IEEE Trans. Antennas Propagat.*, vol. 27, pp. 137-145, Mar. 1979.

[10] W.F. Richards, Y.T. Lo, and D.D. Harrison, "An improved theory for microstrip antennas and applications," *IEEE Trans. Antennas Propagat.*, vol. 29, pp. 38-46, Jan. 1981.

[11] K.R. Carver and J.W. Mink, "Microstrip antenna technology," *IEEE Trans. Antennas Propagat.*, vol. 29, pp. 2-24, Jan. 1981.

[12] C.M. Butler, "Analysis of a coax-fed circular microstrip antenna," in *Proc. Workshop Printed Circuit Antenna Tech.*, New Mexico State Univ., Las Cruces, pp. 13/1-17, Oct. 1979.

[13] R.F. Harrington, *Time-Harmonic Electromagnetic Fields.* New York: McGraw-Hill, 1961, eqn. (3-50).

[14] T.M. Martinson and E.F. Kuester, "The edge admittance of a wide microstrip patch seen by an obliquely incident wave," Scientific Report No. 87, Electromagnetics Laboratory, Department of Electrical and Computer Engineering, University of Colorado, Jan. 1987.

[15] N.N. Lebedev, "The electric field at the edge of a plane condenser containing a dielectric," [Russian], *Zh. Tekh. Fiz.*, vol. 28, pp. 1330-1339, 1958. [Engl. trans. in *Sov. Phys. Tech. Phys.*, vol. 3, pp. 1234-1243, 1958].

[16] W.C. Chew and J.A. Kong, "Asymptotic formula for the capacitance of two oppositely charged discs," *Math. Proc. Camb. Phil. Soc.*, vol. 89, pp. 373-384, 1981.

[17] J. Van Bladel, *Electromagnetic Fields.* Washington: Hemisphere Publishing Corporation, 1985, p. 503.

[18] J. Van Bladel, *Electromagnetic Fields.* Washington: Hemisphere Publishing Corporation, 1985, pp. 45-48.

[19] J.D. Jackson, *Classical Electrodynamics.* New York: Wiley, 1975, pp. 356-360.

[20] A.G. Derneryd, "A theoretical investigation of the rectangular microstrip antenna element," *IEEE Trans. Antennas Propagat.,* vol. 26, pp. 532-535, July 1978.

[21] G. Dubost, "Transmission-line model analysis of a lossy rectangular microstrip patch," *Elect. Letters,* vol. 18, pp. 281-282, Aug. 1982.

[22] E. Lier, "Improved formulas for input impedance of coax-fed microstrip patch antennas," *IEE Proc., pt. H,* vol. 129, pp. 161-164, Aug. 1982.

[23] D.L. Sengupta, "Approximate expression for the resonant frequency of a rectangular patch antenna," *Elect. Letters,* vol. 19, pp. 834-835, Sept. 1983.

[24] I. Wolff and N. Knoppik, "Rectangular and circular microstrip disk capacitors and resonators," *IEEE Trans. Microwave Theory Tech.,* vol. 22, pp. 857-864, Oct. 1974.

[25] Y.T. Lo et al., "Study of microstrip antennas, microstrip phased arrays, and microstrip feed networks," *Final rep. RADC-TR-77-406,* under contract AF19628-76-C-0140, Oct. 1977.

[26] A.G. Derneryd and A.G. Lind, "Extended analysis of rectangular microstrip resonator antennas," *IEEE Trans. Antennas Propagat.,* vol. 27, pp. 846-849, Nov. 1979.

[27] K.R. Carver, "Practical analytical techniques for the microstrip antenna," in *Proc. Workshop Printed Circuit Antenna Tech.,* New Mexico State Univ., Las Cruces, pp. 7/1-19, Oct. 1979.

[28] D.C. Chang, "Analytical theory of an unloaded rectangular microstrip patch," *IEEE Trans. Antennas Propagat.,* vol. 29, pp. 54-62, Jan. 1981.

[29] E.F. Kuester, R.T. Johnk, and D.C. Chang, "The thin-substrate approximation for reflection from the end of a slab-loaded parallel-plate waveguide with application to microstrip patch antennas," *IEEE Trans. Antennas Propagat.,* vol. 30, pp. 910-917, Sept. 1982.

[30] P. Silvester, "Finite element analysis of planar microwave networks," *IEEE Trans. Microwave Theory Tech.,* vol. 21, pp. 104-108, Feb. 1973.

[31] S. Akhtarzad and P.B. Johns, "Three-dimensional transmission-line matrix computer analysis of microstrip resonators", *IEEE Trans. Microwave Theory Tech.,* vol. 23, pp. 990-997, Dec. 1975.

[32] E.H. Newman, P. Tulyathan, "Analysis of microstrip antennas using moment methods", *IEEE Trans. Antennas Propagat.,* vol. 29, pp. 47-53, 1981.

[33] D. Shimin, "A new method for measuring dielectric constant using the resonant frequency of a patch antenna," *IEEE Trans. Microwave Theory Tech.,* vol. 34, pp. 923-931, Sept. 1986.

[34] J. Watkins, "Circular resonant structures in microstrip," *Elect. Letters,* vol. 5, pp. 524-525, Oct. 1969.

[35] E.F. Kuester, "Explicit approximations for the static capacitance of a microstrip patch of arbitrary shape," Scientific Report No. 82, Electromagnetics Laboratory, Department of Electrical and Computer Engineering, University of Colorado, Mar. 1986.

[36] T. Itoh and R. Mittra, "A new method for calculating the capacitance of a circular disk for microwave integrated circuits," *IEEE Trans. Microwave Theory Tech.*, vol. 21, pp. 431-432, June 1973.

[37] S.R. Borkar and R.F.H. Yang, "Capacitance of a circular disk for applications in microwave integrated circuits," *IEEE Trans. Microwave Theory Tech.*, vol. 23, pp. 588-591, July 1975.

[38] S. Coen and G.M.L. Gladwell, "A legendre approximation method for the circular microstrip disk problem," *IEEE Trans. Microwave Theory Tech.*, vol. 25, pp. 1-6, Jan. 1977.

[39] J.R. Mosig, "Les structures microruban: analyse au moyen des équations intégrales," Doctoral Dissertation, Swiss Federal Institute of Technology, Lausanne, Switzerland, 1984.

[40] L.C. Shen et al., "Resonant frequency of a circular disc, printed circuit antenna," *IEEE Trans. Antennas Propagat.*, vol. 25, pp. 595-596, July 1977.

[41] S.A. Long et al., "Impedance of a circular-disc printed-circuit antenna," *Elect. Letters*, vol. 14, pp. 684-686, Oct. 1978.

[42] S.A. Long, L.C. Shen, and P.B. Morel, "Theory of the circular-disc printed-circuit antenna," *Proc. IEE*, vol. 125, pp. 925-928, Oct. 1978.

[43] A.G. Derneryd, "Analysis of the microstrip disk antenna element," *IEEE Trans. Antennas Propagat.*, vol. 27, pp. 660-664, Sept. 1979.

[44] S. Yano and A. Ishimaru, "A theoretical study of the input impedance of a circular microstrip disk antenna," *IEEE Trans. Antennas Propagat.*, vol. 29, pp.77-83, Jan. 1981.

[45] M. Davidovitz and Y.T. Lo, "Input impedance of a probe-fed circular microstrip antenna with thick substrate," *IEEE Trans. Antennas Propagat.*, vol. 34, pp. 905-911, July 1986.

[46] W.C. Chew and J.A. Kong, "Resonance of the axial-symmetric modes in microstrip disk resonators," *J. Math. Phys.*, vol. 21, pp. 582-591, Mar. 1980.

[47] W.C. Chew and J.A. Kong, "Resonance of nonaxial symmetric modes in circular microstrip disk antenna," *J. Math. Phys.*, vol. 21, pp. 2590-2598, Oct. 1980.

[48] W.C. Chew and J.A. Kong, "Asymptotic formula for the resonant frequencies of a circular microstrip antenna," *J. Appl. Phys.*, vol. 52, pp. 5365-5369, Aug. 1981.

[49] W.C. Chew and J.A. Kong, "Analysis of a circular microstrip disk antenna with a thick dielectric substrate," *IEEE Trans. Antennas Propagat.*, vol. 29, pp. 68-76, Jan. 1981.

[50] K. Araki and T. Itoh, "Hankel transform domain analysis of open circular microstrip radiating structures," *IEEE Trans. Antennas Propagat.*, vol. 29, pp. 84-89, Jan. 1981.

[51] C. Wood, "Analysis of microstrip circular patch antennas," *IEE Proc., pt. H*, vol. 128, pp. 69-76, Apr. 1981.

[52] G. Dubost and G. Beauquet, "Linear transmission-line model analysis of a circular patch antenna," *Elect. Letters*, vol. 22, pp. 1174-1176, Oct. 1986.

[53] P.K. Agrawal and M.C. Bailey, "An analysis technique for microstrip antennas," *IEEE Trans. Antennas Propagat.*, vol. 25, pp. 756-759, Nov. 1977.

[54] M.C. Bailey and M.D. Deshpande, "Analysis of elliptical and circular microstrip antennas using moment method," *IEEE Trans. Antennas Propagat.*, vol. 33, pp. 954-959, Sept. 1985.

[55] I.J. Bahl and P. Bhartia, *Microstrip Antennas.* Dedham, MA: Artech House, 1980, pp. 85-105.

[56] M. Abramowitz and I.A. Stegun, editors, *Handbook of mathematical functions.* New York: Dover, 1972, p. 370.

[57] M. Abramowitz and I.A. Stegun, editors, *Handbook of mathematical functions.* New York: Dover, 1972, [17.3.1].

[58] J.R James, P.S. Hall, and C. Wood, *Microstrip antenna - Theory and design.* London: IEE, Peter Peregrinus Ltd., 1981, pp. 74-77.

[59] T.M. Martinson and E.F. Kuester, "Accurate analysis of arbitrarily shaped patch resonators on thin substrates," to be published in *IEEE Trans. Microwave Theory Tech.*, Feb. 1988.

[60] P.M. Morse and H.F. Feshbach, *Methods of Theoretical Physics.* New-York: McGraw-Hill, 1953, pp. 890-891.

[61] P.M. Morse and H.F. Feshbach, *Methods of Theoretical Physics.* New-York: McGraw-Hill, 1953, p. 744.

[62] J.A. Stratton, *Electromagnetic Theory.* New York: McGraw-Hill, 1941, pp. 485-486.

[63] A.K. Rakhmatulina, "Expansion, uniform in a segment, of an integral with decreasing kernel," *USSR Comp. Math. Math. Phys.*, vol. 9, no. 1, pp. 245-256, 1969.

[64] A.N. Tikhonov, A.A. Samarskii and A.A. Arsen'ev, "A method for the asymptotic estimation of integrals," *USSR Comp. Math. Math. Phys.*, vol. 12, no. 4, pp. 196-206, 1972.

[65] M. Abramowitz and I.A. Stegun, editors, *Handbook of mathematical functions.* New York: Dover, 1972, [9.6.4].

[66] I. Gradsteyn and I. Ryzhik, *Tables of Series, Integrals and Products.* New York: Academic Press, 1980, [3.479.2].

[67] M. Abramowitz and I.A. Stegun, editors, *Handbook of mathematical functions.* New York: Dover, 1972, p. 360.

[68] I. Gradsteyn and I. Ryzhik, *Tables of Series, Integrals and Products.* New York: Academic Press, 1980, [6.596.3].

[69] M. Abramowitz and I.A. Stegun, editors, *Handbook of mathematical functions.* New York: Dover, 1972, p. 444.

[70] D.C. Stinson, *Intermediate Mathematics of Electromagnetics.* Englewood Cliffs, NJ: Prentice-Hall, 1976, p. 71.

[71] T.M. Apostol, *Mathematical Analysis.* Reading, MA: Addison-Wesley, 1974, pp. 460-461.

[72] M. Abramowitz and I.A. Stegun, editors, *Handbook of mathematical functions.* New York: Dover, 1972, p. 250.

[73] M. Abramowitz and I.A. Stegun, editors, *Handbook of mathematical functions.* New York: Dover, 1972, [5.2.1] and [5.2.2].

[74] I. Gradsteyn and I. Ryzhik, *Tables of Series, Integrals and Products.* New York: Academic Press, 1980, [2.147.4].

[75] I. Gradsteyn and I. Ryzhik, *Tables of Series, Integrals and Products.* New York: Academic Press, 1980, [2.147.2].

[76] M. Abramowitz and I.A. Stegun, editors, *Handbook of mathematical functions.* New York: Dover, 1972, [5.1.41] and [5.1.42].

[77] M. Abramowitz and I.A. Stegun, editors, *Handbook of mathematical functions.* New York: Dover, 1972, [5.1.1].

[78] M. Abramowitz and I.A. Stegun, editors, *Handbook of mathematical functions.* New York: Dover, 1972, [5.1.43] and [5.1.44].

[79] T.M. Apostol, *Mathematical Analysis.* Reading, MA: Addison-Wesley, 1974, p. 368.

[80] G.N. Watson, *A Treatise on the Theory of Bessel Functions.* Cambridge: Cambridge University Press, 1980, p. 135.

APPENDIX A

In this appendix, we calculate two simple Green functions for the half-space and parallel plate problems. First, G_1 is solution of

$$[\nabla^2 + k_0^2]\, G_1 = -\delta(\bar{r} - \bar{r}') \tag{A1}$$

with a Neumann boundary condition at $z = d$

$$\frac{\partial G_1}{\partial z}\Big|_{z=d} = 0 \quad ; \quad \forall\, \bar{\rho} \tag{A2}$$

We can replace the boundary condition by an image charge at

$$\bar{r}'' = \bar{a}_x\, x' + \bar{a}_y\, y' + \bar{a}_z\,(2d - z')$$

Hence, the Green function G_1 can be replaced by the sum of two free-space Green functions:

$$G_1 = G_1' + G_1''$$

which satisfy

$$[\nabla^2 + k_0^2]\, G_1' = -\delta(\bar{r} - \bar{r}')$$

$$[\nabla^2 + k_0^2]\, G_1'' = -\delta(\bar{r} - \bar{r}'')$$

Thus, we recall the well known free-space Green function [60], and we have

$$4\pi G_1 =$$

$$\frac{e^{-ik_0\left((x-x')^2 + (y-y')^2 + (z-z')^2\right)^{1/2}}}{\left((x-x')^2 + (y-y')^2 + (z-z')^2\right)^{1/2}} + \frac{e^{-ik_0\left((x-x')^2 + (y-y')^2 + (z+z'-2d)^2\right)^{1/2}}}{\left((x-x')^2 + (y-y')^2 + (z+z'-2d)^2\right)^{1/2}} \tag{A3}$$

Second, G_2 is solution of

$$[\nabla^2 + k^2]\, G_2 = -\delta(\bar{r} - \bar{r}') \tag{A4}$$

with a Neumann boundary condition on the interface $z = d$ and ground plane $z = 0$

$$\frac{\partial G_2}{\partial z}\Big|_{z=0,\,d} = 0 \quad ; \quad \forall\, \bar{\rho} \tag{A5}$$

Keeping in mind the boundary condition (A5) and the symmetry of the Green function with respect to z and z', we can express G_2 as a double cosine series:

$$G_2 = \sum_{m=0}^{\infty} \cos\frac{m\pi z}{d} \cos\frac{m\pi z'}{d}\, g_{2m}(x, y\,; x', y') \tag{A6}$$

Then, the wave equation (A4) becomes

$$\sum_{m=0}^{\infty} [k^2 - \frac{m^2\pi^2}{d^2} + \nabla_t^2] \cos\frac{m\pi z}{d} \cos\frac{m\pi z'}{d} g_{2m} = -\delta(x-x')\delta(y-y')\delta(z-z') \qquad \text{(A7)}$$

where ∇_t is the transverse operator

$$\nabla_t = \bar{a}_x \frac{\partial}{\partial x} + \bar{a}_y \frac{\partial}{\partial y}$$

It is a classical procedure to multiply both sides of (A7) by $\cos(n\pi z'/d)$ and then integrate from 0 to d with respect to the variable z'. Then

$$d[\nabla_t^2 - \frac{n^2\pi^2}{d^2} + k^2] g_{2n} = -\epsilon_n \delta(x-x')\delta(y-y') \qquad \text{(A8)}$$

where ϵ_n is the Neumann factor [61]:

$$\epsilon_n = \begin{cases} 1 \; ; \; n = 0 \\ 2 \; ; \; n > 0 \end{cases}$$

Now (A8) is of the generic form

$$[\nabla_t^2 + k^2] A = -\delta(\bar{\rho} - \bar{\rho}') \qquad \text{(A9)}$$

which has a well-known solution [60]:

$$A = -\frac{i}{4} \mathbf{H}_0^{(2)}(k|\bar{\rho} - \bar{\rho}'|) \qquad \text{(A10)}$$

If we compare (A9) and (A10), it follows directly that

$$g_{2m} = -\frac{i\epsilon_m}{4d} \mathbf{H}_0^{(2)}\left((k^2 - \frac{m^2\pi^2}{d^2})^{1/2} |\bar{\rho} - \bar{\rho}'|\right) \qquad \text{(A11)}$$

where the branch of the square root is chosen so as to satisfy the radiation condition [62]:

$$(k^2 - \frac{m^2\pi^2}{d^2})^{1/2} = -i(\frac{m^2\pi^2}{d^2} - k^2)^{1/2} \qquad \text{(A12)}$$

Finally,

$$G_2 = -\frac{i}{4d} \sum_{m=0}^{\infty} \epsilon_m \cos\frac{m\pi z}{d} \cos\frac{m\pi z'}{d} \mathbf{H}_0^{(2)}\left((k^2 - \frac{m^2\pi^2}{d^2})^{1/2} |\bar{\rho} - \bar{\rho}'|\right) \qquad \text{(A13)}$$

APPENDIX B

In this appendix, we accurately approximate the four terms R_{11}, R_{12}, R_{21} and R_{22} given by (30)-(33). Theoretical comments regarding the justification of the approximations can be found in two relevant mathematical papers [63], [64].

Term R_{11}

$$R_{11} = \frac{i\omega\epsilon_0}{2\pi} \int_0^\infty dn' \oint_P dl' \; V(l') E_{0n}(n') \, \hat{a}_{l'} \cdot \oint_P dl \; \Lambda(l) \, \hat{a}_l \; \frac{e^{-ik_0|\vec{\rho} - \vec{\rho}'|}}{|\vec{\rho} - \vec{\rho}'|} \tag{B1}$$

In order to approximate (B1), we simultaneously add and substract a carefully chosen term to the integrand:

$$R_{11} = \frac{i\omega\epsilon_0}{2\pi} \int_0^\infty dn' \oint_P dl' \; V(l') E_{0n}(n') \, \hat{a}_{l'} \cdot \oint_P dl \; \Lambda(l) \, \hat{a}_l \; \frac{e^{-ik_0(|\vec{\rho} - \vec{\rho}_0'|^2 + d^2)^{1/2}}}{(|\vec{\rho} - \vec{\rho}_0'|^2 + d^2)^{1/2}} + \frac{i\omega\epsilon_0}{2\pi} \cdot$$

$$\int_0^\infty dn' \oint_P dl' \; V(l') E_{0n}(n') \, \hat{a}_{l'} \cdot \oint_P dl \; \Lambda(l) \, \hat{a}_l \left[\frac{e^{-ik_0|\vec{\rho} - \vec{\rho}'|}}{|\vec{\rho} - \vec{\rho}'|} - \frac{e^{-ik_0(|\vec{\rho} - \vec{\rho}_0'|^2 + d^2)^{1/2}}}{(|\vec{\rho} - \vec{\rho}_0'|^2 + d^2)^{1/2}} \right] \tag{B2}$$

where $\vec{\rho}_0'(n'=0, l')$ is the point on P corresponding to the point $\vec{\rho}'(n', l')$ as shown in Fig. B1. In splitting the kernel in this way, we have achieved two things. First, the kernel:

$$\frac{e^{-ik_0(|\vec{\rho} - \vec{\rho}_0'|^2 + d^2)^{1/2}}}{(|\vec{\rho} - \vec{\rho}_0'|^2 + d^2)^{1/2}}$$

is independent of n'. Second, the difference kernel:

$$\frac{e^{-ik_0|\vec{\rho} - \vec{\rho}'|}}{|\vec{\rho} - \vec{\rho}'|} - \frac{e^{-ik_0(|\vec{\rho} - \vec{\rho}_0'|^2 + d^2)^{1/2}}}{(|\vec{\rho} - \vec{\rho}_0'|^2 + d^2)^{1/2}}$$

decays very rapidly as source and observation points move apart, since it is of order $(d / |\vec{\rho} - \vec{\rho}'|^2)$ and $(k_0 d / |\vec{\rho} - \vec{\rho}'|)$ when $|\vec{\rho} - \vec{\rho}'| \gg d$ and $n' = O(d)$.

Note that the parameter d introduced in the kernel, the actual height of the substrate, is quite arbitrary at that point. Any small distance of order d, provided we remain consistent from here on would do. However, this particular choice has both advantages of simplifying the calculations and providing a good physical picture. Because of the quick decay of the difference kernel, we can assume that the integrand is of significant magnitude only when $|\vec{\rho} - \vec{\rho}'|$ is small, i.e.

$$\begin{aligned} \hat{a}_l &\simeq \hat{a}_{l'} \\ \Lambda(l) &\simeq \Lambda(l') \end{aligned} \tag{B3}$$

If we substitute (B3) into (B2) and rearrange, then

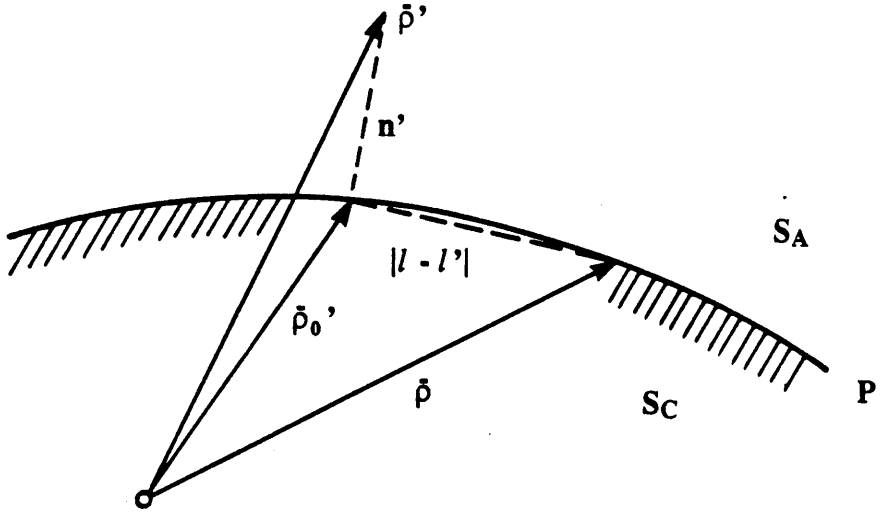

Fig. B1. Edge of the patch.

$$R_{11} = \frac{i\omega\epsilon_0}{2\pi} \int_0^\infty dn'\, E_{0n}(n') \oint_P dl'\, V(l')\, \bar{a}_{l'} \cdot \oint_P dl\, \Lambda(l)\, \bar{a}_l \frac{e^{-ik_0(|\bar{\rho} - \bar{\rho}_0'|^2 + d^2)^{1/2}}}{(|\bar{\rho} - \bar{\rho}_0'|^2 + d^2)^{1/2}}$$

$$+ \frac{i\omega\epsilon_0}{2\pi} \int_0^\infty dn'\, E_{0n}(n') \oint_P dl'\, V(l')\, \Lambda(l') \oint_P dl \left[\frac{e^{-ik_0|\bar{\rho} - \bar{\rho}'|}}{|\bar{\rho} - \bar{\rho}'|} - \frac{e^{-ik_0(|\bar{\rho} - \bar{\rho}_0'|^2 + d^2)^{1/2}}}{(|\bar{\rho} - \bar{\rho}_0'|^2 + d^2)^{1/2}} \right] \tag{B4}$$

The inner integral of the second term in the right-hand side of (B4) is evaluated in Appendix C and thus we can write

$$R_{11} = \frac{i\omega\epsilon_0}{2\pi} \int_0^\infty dn'\, E_{0n}(n') \oint_P dl'\, V(l')\, \bar{a}_{l'} \cdot \oint_P dl\, \Lambda(l)\, \bar{a}_l \frac{e^{-ik_0(|\bar{\rho} - \bar{\rho}_0'|^2 + d^2)^{1/2}}}{(|\bar{\rho} - \bar{\rho}_0'|^2 + d^2)^{1/2}}$$

$$- \frac{i\omega\epsilon_0}{\pi} \int_0^\infty dn'\, E_{0n}(n') \ln\left(\frac{n'}{d}\right) \oint_P dl'\, \Lambda(l')\, V(l') \tag{B5}$$

Term R_{12}

$$R_{12} = \frac{\omega\epsilon_0\epsilon_r}{2d} \sum_{m=1}^{\infty} \int_0^\infty dn$$

$$\cdot \oint_P dl'\, V(l') E_{0n}(n')\, \bar{a}_{l'} \cdot \oint_P dl\, \Lambda(l)\, \bar{a}_l\, \mathbf{H}_0^{(2)}\left(\left(k^2 - \frac{m^2\pi^2}{d^2}\right)^{1/2} |\bar{\rho} - \bar{\rho}'|\right) \tag{B6}$$

Because of the electrically thin substrate, only the dominant parallel-plate mode propagates without attenuation:

$$k^2 < \frac{\pi^2}{d^2}$$

Therefore it is more convenient to write [65]:

$$\mathbf{H}_0^{(2)}\Big(-i\,(\frac{m^2\pi^2}{d^2}-k^2)^{\frac{1}{2}}\,|\bar{\rho}-\bar{\rho}'|\Big)=\frac{2i}{\pi}\,\mathbf{K}_0\Big((\frac{m^2\pi^2}{d^2}-k^2)^{\frac{1}{2}}\,|\bar{\rho}-\bar{\rho}'|\Big) \tag{B7}$$

where $\mathbf{K}_0$ is the modified Bessel function of the second kind of order 0. Since $\mathbf{K}_0$ decays exponentially as its real argument increases, we can use the approximations (B3). Then

$$R_{12}=\frac{i\omega\epsilon_0\epsilon_r}{\pi d}\int_0^\infty dn'\oint_P dl'\;\Lambda(l')\,V(l')\,E_{0n}(n')\sum_{m=1}^{\infty}\oint_P dl\;\mathbf{K}_0\Big((\frac{m^2\pi^2}{d^2}-k^2)^{\frac{1}{2}}\,|\bar{\rho}-\bar{\rho}'|\Big) \tag{B8}$$

The infinite summation is evaluated in Appendix D. We finally have the result

$$R_{12}=-\frac{i\omega\epsilon_0\epsilon_r}{\pi}\int_0^\infty dn'\;E_{0n}(n')\ln(1-e^{-\pi n'/d})\oint_P dl'\;\Lambda(l')\,V(l') \tag{B9}$$

Term $\mathbf{R_{21}}$

$$R_{21}=-\frac{i}{2\pi\omega\mu_0}\int_0^\infty dn'\oint_P dl'\,\frac{\partial V}{\partial l'}H_{0z}(n')\oint_P dl\;\Lambda(l)\,\bar{a}_l\cdot\nabla'\Big[\frac{e^{-ik_0|\bar{\rho}-\bar{\rho}'|}}{|\bar{\rho}-\bar{\rho}'|}\Big] \tag{B10}$$

Directly from the symmetry of the Green function with respect to source and observation points:

$$\nabla' G_1=-\nabla G_1 \tag{B11}$$

We can split the kernel like in (B2). Then, we have

$$R_{21}=\frac{i}{2\pi\omega\mu_0}\int_0^\infty dn'\oint_P dl'\,\frac{\partial V}{\partial l'}H_{0z}(n')\oint_P dl\,\Lambda(l)\frac{\partial}{\partial l}\Big[\frac{e^{-ik_0(|\bar{\rho}-\bar{\rho}_0'|^2+d^2)^{\frac{1}{2}}}}{(|\bar{\rho}-\bar{\rho}_0'|^2+d^2)^{\frac{1}{2}}}\Big]-\frac{i}{2\pi\omega\mu_0}$$

$$\cdot\int_0^\infty dn'\oint_P dl'\,\frac{\partial V}{\partial l'}H_{0z}(n')\oint_P dl\,\Lambda(l)\frac{\partial}{\partial l'}\Big[\frac{e^{-ik_0|\bar{\rho}-\bar{\rho}'|}}{|\bar{\rho}-\bar{\rho}'|}-\frac{e^{-ik_0(|\bar{\rho}-\bar{\rho}_0'|^2+d^2)^{\frac{1}{2}}}}{(|\bar{\rho}-\bar{\rho}_0'|^2+d^2)^{\frac{1}{2}}}\Big] \tag{B12}$$

where we have approximated $\bar{a}_l \simeq \bar{a}_{l'}$ in the second term on the right-hand side because of the quickly decaying kernel. Also, in the same term, we can take the l' derivative out of the inner integral, and then integrate by parts on l'

$$R_{21}=\frac{i}{2\pi\omega\mu_0}\int_0^\infty dn'\;H_{0z}(n')\oint_P dl'\,\frac{\partial V}{\partial l'}\oint_P dl\;\Lambda(l)\frac{\partial}{\partial l}\Big[\frac{e^{-ik_0(|\bar{\rho}-\bar{\rho}_0'|^2+d^2)^{\frac{1}{2}}}}{(|\bar{\rho}-\bar{\rho}_0'|^2+d^2)^{\frac{1}{2}}}\Big]$$

$$-\frac{i}{\pi\omega\mu_0}\int_0^\infty dn'\, H_{0z}(n')\ln\left(\frac{n'}{d}\right)\oint_P dl'\, \Lambda(l')\frac{\partial^2 V}{\partial l'^2} \tag{B13}$$

Because of the rapidly decaying kernel, we have substituted $\Lambda(l)$ for $\Lambda(l')$. We also have recalled the result of Appendix C for the inner integral of the second term in the right-hand side of (B13).

Term $\mathbf{R_{22}}$

$$R_{22} = \frac{-i}{\pi\omega\mu_0\mu_r d}\sum_{m=1}^{\infty}\int_0^\infty dn'$$

$$\cdot \oint_P dl'\,\frac{\partial V}{\partial l'} H_{0z}(n')\oint_P dl\,\Lambda(l)\,\bar{a}_l\cdot\nabla'\left[\mathbf{K}_0\left(\left(\frac{m^2\pi^2}{d^2}-k^2\right)^{1/2}|\bar{\rho}-\bar{\rho}'|\right)\right] \tag{B14}$$

Again because of the rapidly decaying kernel in the inner integral, we can use the approximation (B3). Then, we obtain

$$R_{22} = \frac{-i}{\pi\omega\mu_0\mu_r d}$$

$$\cdot \sum_{m=0}^{\infty}\int_0^\infty dn'\, H_{0z}(n')\oint_P dl'\,\frac{\partial V}{\partial l'}\frac{\partial}{\partial l'}\oint_P dl\,\Lambda(l)\mathbf{K}_0\left(\left(\frac{m^2\pi^2}{d^2}-k^2\right)^{1/2}|\bar{\rho}-\bar{\rho}'|\right) \tag{B15}$$

We can integrate the above expression by parts with respect to l'

$$R_{22} = -\frac{i}{\pi\omega\mu_0\mu_r}\int_0^\infty dn'\, H_{0z}(n')\ln\left(1-e^{-\pi n'/d}\right)\oint_P dl'\,\Lambda(l')\frac{\partial^2 V}{\partial l'^2} \tag{B16}$$

where we have called back the result for the inner integral developed in Appendix D.

APPENDIX C

In this appendix, we derive an accurate approximation for the integral

$$I = \oint_P dl \left[\frac{e^{-ik_0|\bar{\rho} - \bar{\rho}'|}}{|\bar{\rho} - \bar{\rho}'|} - \frac{e^{-ik_0(|\bar{\rho} - \bar{\rho}_0'|^2 + d^2)^{1/2}}}{(|\bar{\rho} - \bar{\rho}_0'|^2 + d^2)^{1/2}} \right] \tag{C1}$$

The integrand is rapidly decaying as $|\bar{\rho} - \bar{\rho}'|$ increases. Thus, we can justify the following approximations (see fig. B1):

$$|\bar{\rho} - \bar{\rho}'| \simeq \left((l - l')^2 + n'^2\right)^{1/2} \tag{C2}$$

$$|\bar{\rho} - \bar{\rho}_0'| \simeq |l - l'| \tag{C3}$$

Also because of this rapid decay of the kernel, we can safely extend the integration limits from $l = -\infty$ to $l = \infty$. It follows that (C1) becomes

$$I = \int_{-\infty}^{\infty} dl \left[\frac{e^{-ik_0((l - l')^2 + n'^2)^{1/2}}}{((l - l')^2 + n'^2)^{1/2}} - \frac{e^{-ik_0((l - l')^2 + d^2)^{1/2}}}{((l - l')^2 + d^2)^{1/2}} \right] \tag{C4}$$

At this point, we recall an integral representation of the Hankel function of the first kind of order zero [66]:

$$i\pi \, \mathbf{H}_0^{(1)}(\mu) = \int_{-\infty}^{\infty} dx \, \frac{e^{i\mu\sqrt{1 + x^2}}}{\sqrt{1 + x^2}} \tag{C5}$$

Therefore,

$$\int_{-\infty}^{\infty} dl \, \frac{e^{-ik_0((l - l')^2 + n'^2)^{1/2}}}{((l - l')^2 + n'^2)^{1/2}} = i\pi \, \mathbf{H}_0^{(1)}(-k_0 n') = -i\pi \, \mathbf{H}_0^{(2)}(k_0 n') \tag{C6}$$

We now use the result (C6) into the expression (C4):

$$I = i\pi \left\{ \mathbf{H}_0^{(2)}(k_0 d) - \mathbf{H}_0^{(2)}(k_0 n') \right\} \tag{C7}$$

Furthermore, since both $k_0 d$ and $k_0 n'$ are small in the range where the integrand is significant, we can use the small argument expansion for the Hankel function [67]:

$$\mathbf{H}_0^{(2)}(z) = 1 - \frac{2i}{\pi}\left(\ln \frac{z}{2} + \gamma\right) + \mathrm{O}(z^2 \ln z)$$

and we finally have

$$I = -2 \ln\left(\frac{n'}{d}\right) \tag{C8}$$

APPENDIX D

In this appendix, we derive an accurate approximation for the summation

$$S = \sum_{m=1}^{\infty} \oint_P dl\ \mathbf{K}_0\Big(\big(\frac{m^2\pi^2}{d^2} - k^2\big)^{1/2}\ |\tilde{\rho} - \tilde{\rho}'|\Big) \tag{D1}$$

Because of the exponential decay along the real axis as $|\tilde{\rho} - \tilde{\rho}'|$ increases, we can justify the following approximation (see fig. B1):

$$|\tilde{\rho} - \tilde{\rho}'| \simeq ((l - l')^2 + n'^2)^{1/2} \tag{D2}$$

Also, with the same kind of approximation, we can extend the integration limits from $l = -\infty$ to $l = \infty$

$$S = \sum_{m=1}^{\infty} \int_{-\infty}^{\infty} dl\ \mathbf{K}_0\Big(\big(\frac{m^2\pi^2}{d^2} - k^2\big)^{1/2}\ ((l - l')^2 + n'^2)^{1/2}\Big) \tag{D3}$$

Recall the following result [68]:

$$\int_{-\infty}^{\infty} dx\ \mathbf{K}_0(\alpha\sqrt{x^2 + z^2}\ ) = \frac{\pi}{\alpha}\ e^{-\alpha z} \tag{D4}$$

where we have used the identity [69]:

$$\mathbf{K}_{-1/2}(\alpha z) = \left(\frac{\pi}{2\alpha z}\right)^{1/2} e^{-\alpha z}$$

The summation S can now be rewritten as follows

$$S = \sum_{m=1}^{\infty} \frac{\pi}{\big(\frac{m^2\pi^2}{d^2} - k^2\big)^{1/2}}\ e^{-\big(\frac{m^2\pi^2}{d^2} - k^2\big)^{1/2} n'} \tag{D5}$$

Using small kd approximation,

$$\big(\frac{m^2\pi^2}{d^2} - k^2\big)^{1/2} \simeq \frac{m\pi}{d}$$

we have the result

$$S = \sum_{m=1}^{\infty} \frac{d}{m}\ e^{-\frac{m\pi n'}{d}} = -d\ln(1 - e^{-\pi n'/d}) \tag{D6}$$

APPENDIX E

In this appendix, we will derive a small $(k_0 d)$ approximation of the integral I_{11}

$$I_{11} = \int_0^{l_x} dx \int_0^{l_x} dx' \cos\tilde{k}x \cos\tilde{k}x' \frac{e^{-ik_0\left((x-x')^2 + d^2\right)^{1/2}}}{\left((x-x')^2 + d^2\right)^{1/2}} \tag{E1}$$

We first recall a well-known spectral representation of the kernel [70]:

$$\frac{e^{-ik_0\left((x-x')^2 + d^2\right)^{1/2}}}{\left((x-x')^2 + d^2\right)^{1/2}} = -\frac{i}{2}\int_{-\infty}^{\infty} d\lambda \; \mathbf{H}_0^{(2)}\left(d\,(k_0^2 - \lambda^2)^{1/2}\right) e^{-i\lambda(x-x')} \tag{E2}$$

with the branch of the square root defined as

$$\mathrm{Im}\left[d(k_0^2 - \lambda^2)^{1/2}\right] \leq 0 \tag{E3}$$

The integration path in the complex λ—*plane* is shown in Fig. E1. Note that the proper sheet is defined by the condition (E3). Remark also that the logarithmic branch cut in the $(k_0^2 - \lambda^2)^{1/2}$ —*plane* maps into the square root branch cuts in the λ—*plane*, so that there is no additional branch cut. (Fig. E2). Now introduce the spectral representation (E2) into expression (E1) and interchange the integrals to obtain

$$I_{11} = -\frac{i}{2}\int_{-\infty}^{\infty} d\lambda \; \mathbf{H}_0^{(2)}\left(d\,(k_0^2 - \lambda^2)^{1/2}\right) \int_0^{l_x} dx \cos\tilde{k}x \; e^{-i\lambda x} \int_0^{l_x} dx' \cos\tilde{k}x' \; e^{i\lambda x'} \tag{E4}$$

We can easily calculate the x and x' integrals

$$\int_0^{l_x} dx \cos\tilde{k}x \; e^{-i\lambda x} = \frac{i\lambda\left(1 + e^{-i\lambda l_x}\right)}{\tilde{k}^2 - \lambda^2} \tag{E5}$$

Thus,

$$I_{11} = -i\int_{-\infty}^{\infty} d\lambda \; \mathbf{H}_0^{(2)}\left(d\,(k_0^2 - \lambda^2)^{1/2}\right) \frac{\lambda^2\left(1 + \cos\lambda l_x\right)}{\left(\tilde{k}^2 - \lambda^2\right)^2} \tag{E6}$$

Since, by hypothesis, $(k_0 d) \ll 1$, we can presumably use the small argument expansion of the Hankel function [67]:

$$\mathbf{H}_0^{(2)}\left(d\,(k_0^2 - \lambda^2)^{1/2}\right) = H - \frac{2i}{\pi}\ln\left(k_0^2 - \lambda^2\right)^{1/2} + \mathrm{O}\left((k_0 d)^2 \ln(k_0 d)\right) \tag{E7}$$

where we have defined the constant

$$H = 1 - \frac{2i}{\pi}\left(\gamma + \ln(d/2)\right) \tag{E8}$$

and γ is Euler's constant 0.57721... Therefore, we can split I_{11} into four terms:

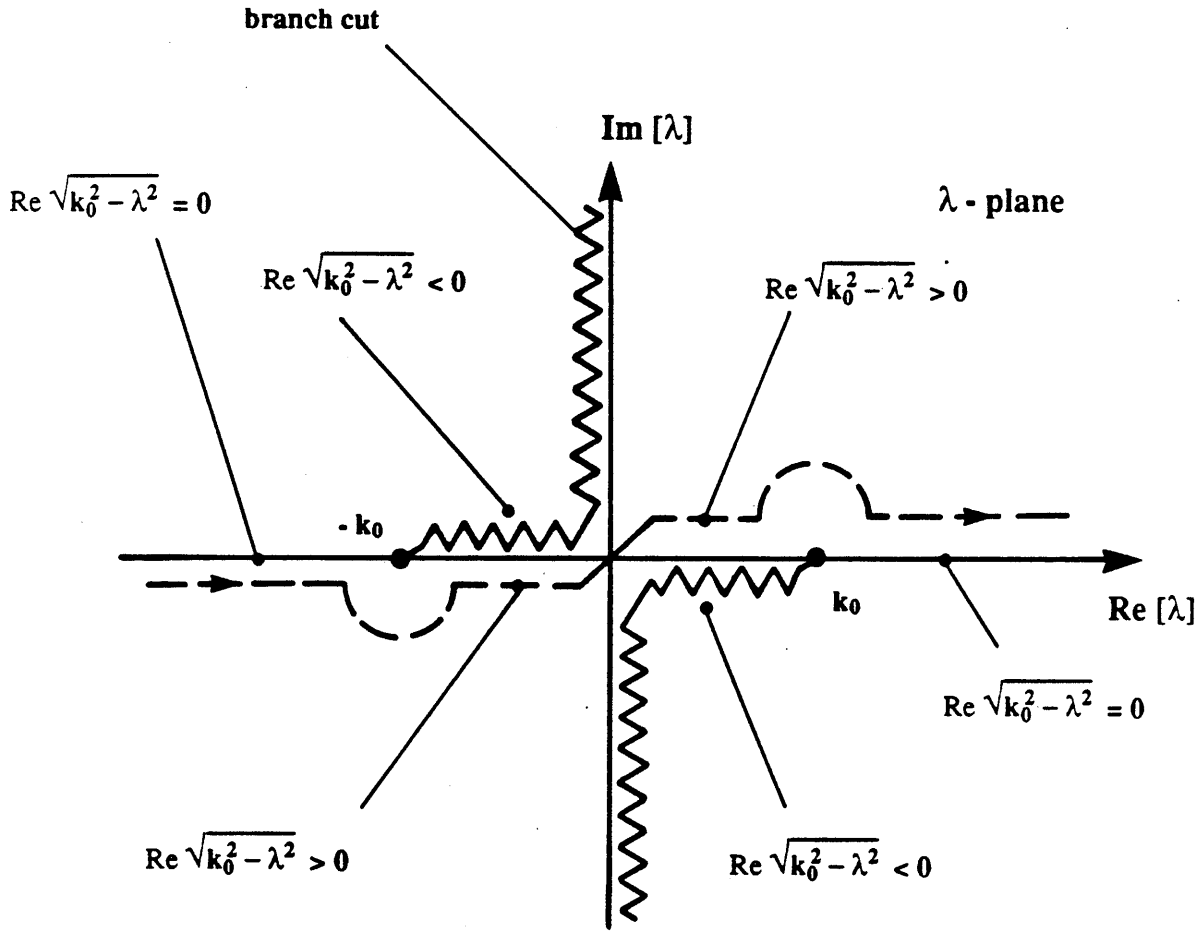

Fig. E1. Situation in the λ-plane.

$$I_{11} = -iH\,(I_A + I_B) - \frac{2}{\pi}\,(I_C + I_D) \tag{E9}$$

where

$$I_A = \int_{-\infty}^{\infty} d\lambda \frac{\lambda^2}{(\tilde{k}^2 - \lambda^2)^2} \tag{E10}$$

$$I_B = \int_{-\infty}^{\infty} d\lambda \frac{\lambda^2 \cos \lambda l_x}{(\tilde{k}^2 - \lambda^2)^2} \tag{E11}$$

$$I_C = \int_{-\infty}^{\infty} d\lambda \ln(k_0^2 - \lambda^2)^{\frac{1}{2}} \frac{\lambda^2}{(\tilde{k}^2 - \lambda^2)^2} \tag{E12}$$

$$I_D = \int_{-\infty}^{\infty} d\lambda \ln(k_0^2 - \lambda^2)^{\frac{1}{2}} \frac{\lambda^2 \cos \lambda l_x}{(\tilde{k}^2 - \lambda^2)^2} \tag{E13}$$

along the integration path shown in Fig. E1.

Integral I_A

By direct application of the Residue Theorem [71]:

$$I_A = \int_{-\infty}^{\infty} d\lambda \frac{\lambda^2}{(\tilde{k}^2 - \lambda^2)^2} = -2\pi i \underset{\lambda = \tilde{k}}{Res} \left[\frac{\lambda^2}{(\tilde{k}^2 - \lambda^2)^2}\right] = -\frac{i\pi}{2\tilde{k}} \tag{E14}$$

Integral I_B

We can rewrite I_B as

$$I_B = \int_{-\infty}^{\infty} d\lambda \frac{\lambda^2 \cos \lambda l_x}{(\tilde{k}^2 - \lambda^2)^2} = \int_{-\infty}^{\infty} d\lambda \frac{\lambda^2 e^{i\lambda l_x}}{(\tilde{k}^2 - \lambda^2)^2} \tag{E15}$$

We also use the residue theorem, closing the contour in the upper half-plane,

$$I_B = 2\pi i \underset{\lambda = -\tilde{k}}{Res} \left[\frac{\lambda^2 e^{i\lambda l}}{(\tilde{k}^2 - \lambda^2)^2}\right] = \frac{i\pi e^{-i\tilde{k}l_x}}{2\tilde{k}} (i\tilde{k}l_x - 1) \tag{E16}$$

Integral I_C

$$I_C = \int_{-\infty}^{\infty} d\lambda \ln(k_0^2 - \lambda^2)^{\frac{1}{2}} \frac{\lambda^2}{(\tilde{k}^2 - \lambda^2)^2}$$

Again, we choose to use the Residue Theorem, closing the contour in the upper half-plane. This time, we get both a residue and a branch cut contribution, as shown in Fig. E3.

$$\begin{aligned} I_C &= 2\pi i \underset{\lambda = -\tilde{k}}{Res} \left[\frac{\ln(k_0^2 - \lambda^2)^{\frac{1}{2}} \lambda^2}{(\tilde{k}^2 - \lambda^2)^2}\right] + I_{bc} \\ &= \frac{i\pi\tilde{k}}{2(k_0^2 - \tilde{k}^2)} - \frac{i\pi \ln(k_0^2 - \tilde{k}^2)^{\frac{1}{2}}}{2\tilde{k}} + I_{bc} \end{aligned} \tag{E17}$$

where the branch cut integral is given by

$$I_{bc} = \int_{-\infty}^{-k_0} ds \frac{-s(k_0^2 - s^2)\ln s}{i(s^2 - k_0^2)^{\frac{1}{2}}(s^2 - k_0^2 + \tilde{k}^2)^2} + \int_{-k_0}^{0} ds \frac{s(k_0^2 - s^2)\ln s}{(k_0^2 - s^2)^{\frac{1}{2}}(s^2 - k_0^2 + \tilde{k}^2)^2}$$

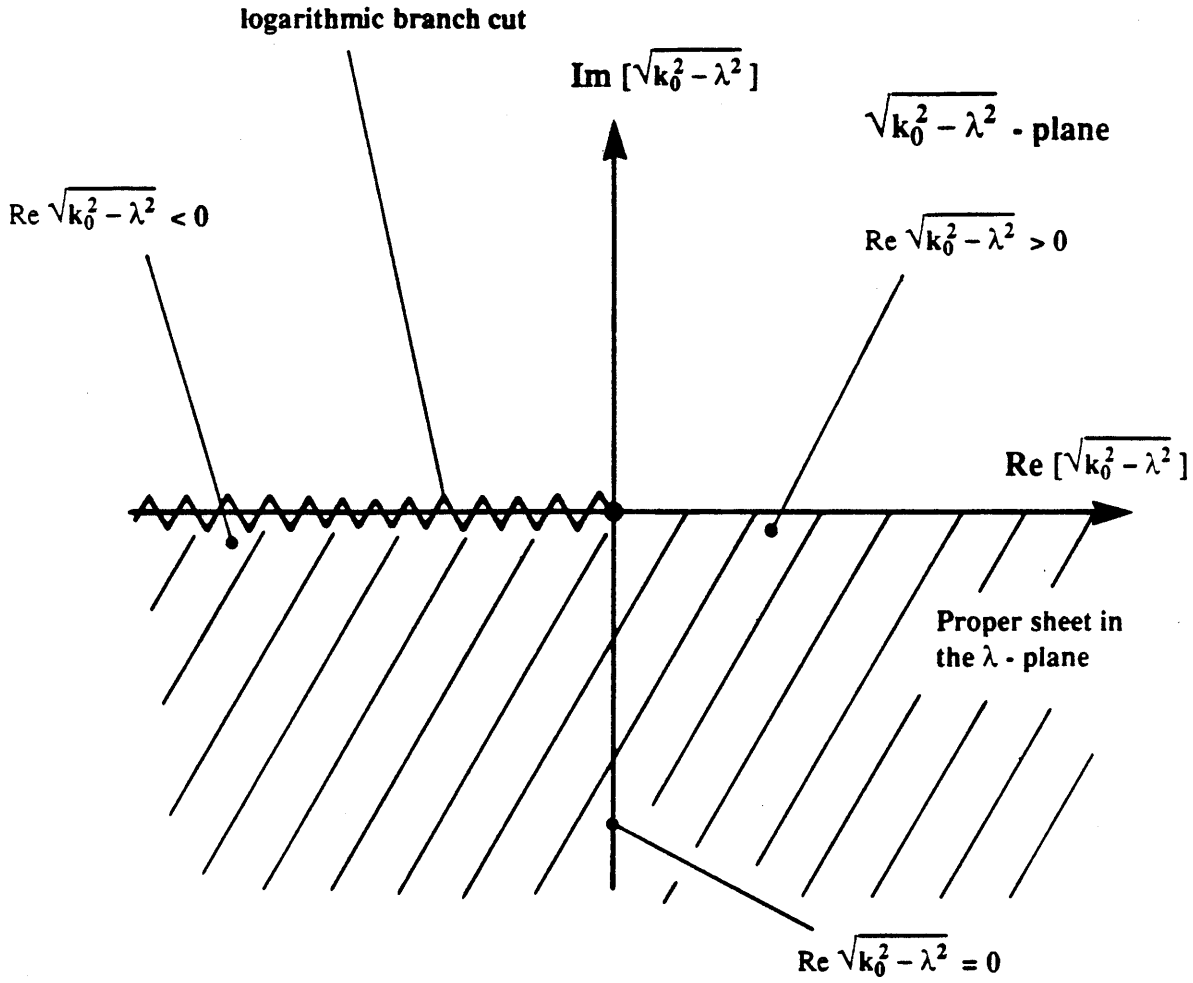

Fig. E2. Situation in the $(k_0^2 - \lambda^2)^{1/2}$ - plane.

$$+ \int_0^{k_0} ds \frac{s(k_0^2 - s^2)\ln s}{(k_0^2 - s^2)^{1/2}(s^2 - k_0^2 + \tilde{k}^2)^2} + \int_{k_0}^{\infty} ds \frac{-s(k_0^2 - s^2)\ln s}{i(s^2 - k_0^2)^{1/2}(s^2 - k_0^2 + \tilde{k}^2)^2}$$

and s is a real parameter along the branch cut defined as

$$s = (k_0^2 - \lambda^2)^{1/2} \tag{E18}$$

To stay on the proper sheet, we require

$$arg\,(s) = -\pi \quad \text{if } s < 0 \tag{E19}$$

After some straightforward manipulations,

$$I_{bc} = i\pi \int_0^{k_0} ds\, \frac{s\,(k_0^2 - s^2)^{1/2}}{(s^2 - k_0^2 + \tilde{k}^2)^2} + \pi \int_{k_0}^{\infty} ds\, \frac{s\,(s^2 - k_0^2)^{1/2}}{(s^2 - k_0^2 + \tilde{k}^2)^2} \tag{E20}$$

These two integrals are computed in appendix F,

$$\int_0^{k_0} ds\, \frac{s\,(k_0^2 - s^2)^{1/2}}{(s^2 - k_0^2 + \tilde{k}^2)^2} = \frac{k_0}{2(\tilde{k}^2 - k_0^2)} - \frac{1}{4\tilde{k}} \ln\left(\frac{\tilde{k} + k_0}{\tilde{k} - k_0}\right) \tag{E21}$$

and,

$$\int_{k_0}^{\infty} ds\, \frac{s\,(s^2 - k_0^2)^{1/2}}{(s^2 - k_0^2 + \tilde{k}^2)^2} = \frac{\pi}{4\tilde{k}} \tag{E22}$$

The branch cut contribution can now be written in closed form:

$$I_{bc} = \frac{i\pi k_0}{2(\tilde{k}^2 - k_0^2)} - \frac{i\pi}{4\tilde{k}} \ln\left(\frac{\tilde{k} + k_0}{\tilde{k} - k_0}\right) + \frac{\pi^2}{4\tilde{k}} \tag{E23}$$

Adding the residue contribution, we write

$$I_C = -\frac{i\pi}{2}\left[\frac{1}{\tilde{k} + k_0} + \frac{\ln(k_0^2 - \tilde{k}^2)^{1/2}}{\tilde{k}} + \frac{1}{2\tilde{k}} \ln\left(\frac{\tilde{k} + k_0}{\tilde{k} - k_0}\right) + \frac{i\pi}{2\tilde{k}}\right] \tag{E24}$$

On the proper sheet of the λ–*plane*,

$$\ln(k_0^2 - \tilde{k}^2)^{1/2} = -\frac{i\pi}{2} + \frac{1}{2} \ln(\tilde{k}^2 - k_0^2) \tag{E25}$$

Thus, we finally have

$$I_c = -\frac{i\pi}{2}\left[\frac{1}{\tilde{k} + k_0} + \frac{\ln(\tilde{k} + k_0)}{\tilde{k}}\right] \tag{E26}$$

Integral I_D

We can rewrite I_D as

$$I_D = \int_{-\infty}^{\infty} d\lambda \ln(k_0^2 - \lambda^2)^{1/2} \frac{\lambda^2 \cos\lambda l_z}{(\tilde{k}^2 - \lambda^2)^2} = \int_{-\infty}^{\infty} d\lambda \ln(k_0^2 - \lambda^2)^{1/2} \frac{\lambda^2 e^{i\lambda l_z}}{(\tilde{k}^2 - \lambda^2)^2} \tag{E27}$$

We close the contour in the upper half-plane, to obtain

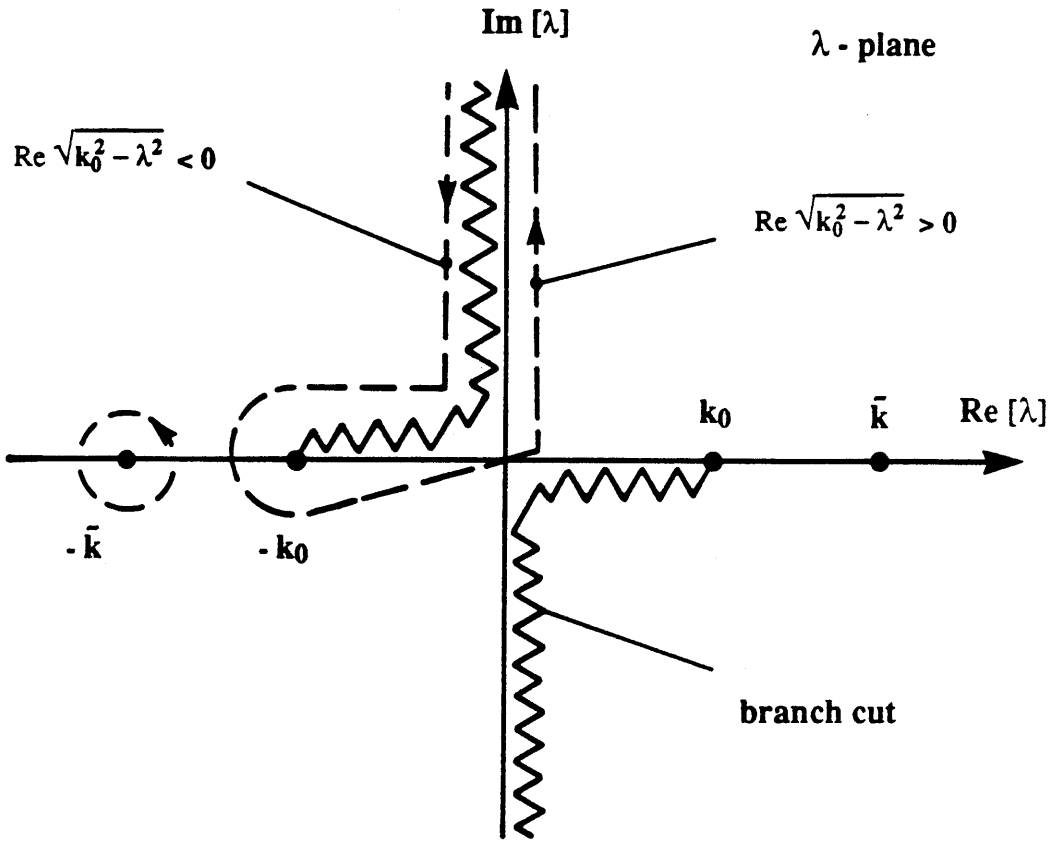

Fig. E3. Integration contour.

$$I_D = 2\pi i \operatorname*{Res}_{\lambda=-\tilde{k}} \left[\ln(k_0^2 - \lambda^2)^{1/2} \frac{\lambda^2 e^{i\lambda l_z}}{(\tilde{k}^2 - \lambda^2)^2} \right] + I_{bc}$$

$$= -\frac{i\pi}{2\tilde{k}} \left[\frac{\tilde{k}^2 e^{-i\tilde{k}l_z}}{\tilde{k}^2 - k_0^2} + \left[i\pi - \ln(\tilde{k}^2 - k_0^2) \right] e^{-i\tilde{k}l_z} \frac{(i\tilde{k}l_z - 1)}{2} \right] + I_{bc} \qquad \text{(E28)}$$

where

$$I_{bc} = \int_{-\infty}^{-k_0} ds \frac{-s \ln s \, (k_0^2 - s^2) \, e^{-(s^2 - k_0^2)^{1/2} l_z}}{i(s^2 - k_0^2)^{1/2} (s^2 - k_0^2 + \tilde{k}^2)^2} + \int_{-k_0}^{0} ds \frac{s \ln s \, (k_0^2 - s^2) \, e^{-i(k_0^2 - s^2)^{1/2} l_z}}{(k_0^2 - s^2)^{1/2} (s^2 - k_0^2 + \tilde{k}^2)^2}$$

$$+\int_0^{k_0} ds\,\frac{s\ln s\,(k_0^2-s^2)\,e^{-i(k_0^2-s^2)^{1/2}l_z}}{(k_0^2-s^2)^{1/2}(s^2-k_0^2+\tilde{k}^2)^2}+\int_{k_0}^{\infty} ds\,\frac{-s\ln s\,(k_0^2-s^2)\,e^{-(s^2-k_0^2)^{1/2}l_z}}{i\,(s^2-k_0^2)^{1/2}\,(s^2-k_0^2+\tilde{k}^2)^2} \tag{E29}$$

with s defined as in (E18) and (E19). We find

$$I_{bc}=i\pi\int_0^{k_0} ds\,\frac{s\,(k_0^2-s^2)^{1/2}\,e^{-i(k_0^2-s^2)^{1/2}l_z}}{(s^2-k_0^2+\tilde{k}^2)^2}+\pi\int_{k_0}^{\infty} ds\,\frac{s\,(s^2-k_0^2)^{1/2}\,e^{-(s^2-k_0^2)^{1/2}l_z}}{(s^2-k_0^2+\tilde{k}^2)^2} \tag{E30}$$

Again, these two integrals can be computed in closed form (appendix F).

$$\int_0^{k_0} ds\,\frac{s\,(k_0^2-s^2)^{1/2}\,e^{-i(k_0^2-s^2)^{1/2}l_z}}{(s^2-k_0^2+\tilde{k}^2)^2}=\frac{k_0\,e^{-ik_0l_z}}{2(\tilde{k}^2-k_0^2)}$$

$$+\frac{(i\tilde{k}l_z-1)}{4\tilde{k}}\,e^{-i\tilde{k}l_z}\left[E_1(-i\tilde{k}l_z+ik_0l_z)-E_1(-i\tilde{k}l_z)\right]$$

$$+\frac{(i\tilde{k}l_z+1)}{4\tilde{k}}\,e^{i\tilde{k}l_z}\left[E_1(i\tilde{k}l_z+ik_0l_z)-E_1(i\tilde{k}l_z)\right] \tag{E31}$$

and,

$$\int_{k_0}^{\infty} ds\,\frac{s\,(s^2-k_0^2)^{1/2}\,e^{-(s^2-k_0^2)^{1/2}l_z}}{(s^2-k_0^2+\tilde{k}^2)^2}=$$

$$-\frac{\mathrm{Im}\left[e^{i\tilde{k}l_z}\,E_1(i\tilde{k}l_z)\right]}{2\tilde{k}}-\frac{l_z\,\mathrm{Re}\left[e^{i\tilde{k}l_z}\,E_1(i\tilde{k}l_z)\right]}{2} \tag{E32}$$

Then the result comes in a straightforward way

$$I_D=-\frac{i\pi}{2\tilde{k}}\left[\frac{\tilde{k}^2\,e^{-i\tilde{k}l_z}}{\tilde{k}^2-k_0^2}+\left[i\pi-\ln(\tilde{k}^2-k_0^2)\right]e^{-i\tilde{k}l_z}\,\frac{(i\tilde{k}l_z-1)}{2}\right]$$

$$+\frac{i\pi k_0\,e^{-ik_0l_z}}{2(\tilde{k}^2-k_0^2)}+\frac{i\pi}{4\tilde{k}}(i\tilde{k}l_z-1)\,e^{-i\tilde{k}l_z}\left[E_1(-i\tilde{k}l_z+ik_0l_z)-E_1(-i\tilde{k}l_z)\right]$$

$$+\frac{i\pi}{4\tilde{k}}(i\tilde{k}l_z+1)\,e^{i\tilde{k}l_z}\left[E_1(i\tilde{k}l_z+ik_0l_z)-E_1(i\tilde{k}l_z)\right]$$

$$-\frac{\pi}{2\tilde{k}}\mathrm{Im}\left[e^{i\tilde{k}l_z}\,E_1(i\tilde{k}l_z)\right]-\frac{\pi l_z}{2}\mathrm{Re}\left[e^{i\tilde{k}l_z}\,E_1(i\tilde{k}l_z)\right] \tag{E33}$$

Putting all the pieces together according to equation (E9), we eventually obtain

$$I_{11}=-\frac{\pi H}{2\tilde{k}}+\frac{\pi H\,e^{-i\tilde{k}l_z}}{2\tilde{k}}(i\tilde{k}l_z-1)+\frac{\mathrm{Im}\left[e^{i\tilde{k}l_z}\,E_1(i\tilde{k}l_z)\right]}{\tilde{k}}+l_z\,\mathrm{Re}\left[e^{i\tilde{k}l_z}\,E_1(i\tilde{k}l_z)\right]$$

$$+ i \Bigg(\frac{1}{\tilde{k} + k_0} + \frac{\ln(\tilde{k} + k_0)}{\tilde{k}} + \frac{\tilde{k}\ e^{-i\tilde{k}l_z} - k_0\ e^{-ik_0 l_z}}{\tilde{k}^2 - k_0^2}$$

$$+ (i\tilde{k}l_z - 1)\left[i\pi - \ln(\tilde{k}^2 - k_0^2)\right] \frac{e^{-i\tilde{k}l_z}}{2\tilde{k}}$$

$$+ \frac{(1 - i\tilde{k}l_z)}{2\tilde{k}}\ e^{-i\tilde{k}l_z}\ \left[E_1(-i\tilde{k}l_z + ik_0 l_z) - E_1(-i\tilde{k}l_z)\right]$$

$$- \frac{(1 + i\tilde{k}l_z)}{2\tilde{k}}\ e^{i\tilde{k}l_z}\ \left[E_1(\ i\tilde{k}l_z + ik_0 l_z) - E_1(\ i\tilde{k}l_z)\right] \Bigg) \qquad \text{(E34)}$$

Recall that $\tilde{k} = \pi/l_z$ and that [72]

$$E_1(i\pi) = \ - Ci\,(\pi) + i\,Si\,(\pi) - \frac{i\pi}{2}$$

$$E_1(-i\pi) = \ - Ci\,(\pi) - i\,Si\,(\pi) + \frac{i\pi}{2} \qquad \text{(E35)}$$

where the sine integral and cosine integral functions are defined in [73]:

$$Si\,(x) = \int_0^x dt\ \frac{\sin t}{t} \qquad \text{(E36)}$$

$$Ci\,(x) = \gamma + \ln x + \int_0^x dt\ \frac{\cos t - 1}{t} \qquad \text{(E37)}$$

We therefore can write the result, exact in the limit $(k_0 d) \rightarrow 0$,

$$I_{11} = l_z\ Ci(\pi) - \frac{Si(\pi)}{\tilde{k}} - \frac{\pi}{\tilde{k}}\,(\gamma + \ln(d/2)) - \frac{\pi \ln(\tilde{k}^2 - k_0^2)}{2\tilde{k}}$$

$$+ i\left[\frac{1}{\tilde{k} + k_0} - \frac{\tilde{k} + k_0\ e^{-ik_0 l_z}}{\tilde{k}^2 - k_0^2} + \frac{1}{2\tilde{k}} \ln\left(\frac{\tilde{k} + k_0}{\tilde{k} - k_0}\right)\right] - \frac{(i + \pi)}{2\tilde{k}}\ E_1(ik_0 l_z - i\pi)$$

$$+ \frac{(i - \pi)}{2\tilde{k}}\ E_1(ik_0 l_z + i\pi) + \frac{Si\,(\pi) - \pi/2 - \pi\,Ci\,(\pi)}{\tilde{k}} \qquad \text{(E38)}$$

APPENDIX F

In this appendix, we calculate four integrals needed in appendix E.

First Integral

$$\int_0^{k_0} ds\, \frac{s\,(k_0^2 - s^2)^{1/2}}{(s^2 - k_0^2 + \tilde{k}^2)^2} = \int_0^{k_0} dt\, \frac{t^2}{(t^2 - \tilde{k}^2)^2} = \frac{1}{\tilde{k}} \int_0^{k_0/\tilde{k}} dx\, \frac{x^2}{(1-x^2)^2}$$

The last integral is known in closed form [74]:

$$\int dx\, \frac{x^2}{(1-x^2)^2} = \frac{x}{2(1-x^2)} - \frac{1}{4} \ln\Big(\frac{1+x}{1-x}\Big)$$

Therefore,

$$\int_0^{k_0} ds\, \frac{s\,(k_0^2 - s^2)^{1/2}}{(s^2 - k_0^2 + \tilde{k}^2)^2} = \frac{k_0}{2(\tilde{k}^2 - k_0^2)} - \frac{1}{4\tilde{k}} \ln\Big(\frac{\tilde{k} + k_0}{\tilde{k} - k_0}\Big) \tag{F1}$$

Second Integral

$$\int_{k_0}^{\infty} ds\, \frac{s\,(s^2 - k_0^2)^{1/2}}{(s^2 - k_0^2 + \tilde{k}^2)^2} = \int_0^{\infty} dt\, \frac{t^2}{(t^2 + \tilde{k}^2)^2} = \frac{1}{\tilde{k}} \int_0^{\infty} dx\, \frac{x^2}{(1+x^2)^2}$$

Recall another tabulated result [75]:

$$\int dx\, \frac{x^2}{(1+x^2)^2} = \frac{-x}{2(1+x^2)} + \frac{1}{2} \tan^{-1} x$$

Thus, we obtain the result:

$$\int_{k_0}^{\infty} ds\, \frac{s\,(s^2 - k_0^2)^{1/2}}{(s^2 - k_0^2 + \tilde{k}^2)^2} = \frac{\pi}{4\tilde{k}} \tag{F2}$$

Third Integral

$$\int_0^{k_0} ds\, \frac{s\,(k_0^2 - s^2)^{1/2}\, e^{-i(k_0^2 - s^2)^{1/2} l_z}}{(s^2 - k_0^2 + \tilde{k}^2)^2} = \int_0^{k_0} dx\, \frac{x^2\, e^{-ix\, l_z}}{(x^2 - \tilde{k}^2)^2}$$

Integrate by parts to find

$$= -\frac{k_0\, e^{-ik_0 l_z}}{2(k_0^2 - \tilde{k}^2)} + \int_0^{k_0} dx\, \frac{e^{-ix\,l_z}\,(1 - ix\,l_z)}{2(x^2 - \tilde{k}^2)}$$

We need two tabulated integrals [76]:

$$\int dx\, \frac{e^{ix}}{a^2 + x^2} = \frac{i}{2a}\left[e^{-a}\,E_1(-a-ix) - e^{a}\,E_1(a-ix)\right]$$

$$\int dx\, \frac{x\,e^{ix}}{a^2 + x^2} = -\frac{1}{2}\left[e^{-a}\,E_1(-a-ix) + e^{a}\,E_1(a-ix)\right]$$

where the exponential integral E_1 is defined by [77]:

$$E_1(z) = \int_z^{\infty} dt\, \frac{e^{-t}}{t} \qquad (|\,arg\ z\,| < \pi)$$

It is now an easy matter to get the result:

$$\int_0^{k_0} ds\, \frac{s\,(k_0^2 - s^2)^{1/2}\, e^{-i(k_0^2 - s^2)^{1/2} l_z}}{(s^2 - k_0^2 + \tilde{k}^2)^2} = \frac{k_0\, e^{-ik_0 l_z}}{2(\tilde{k}^2 - k_0^2)}$$

$$+ \frac{(i\tilde{k}l_z - 1)}{4\tilde{k}}\, e^{-i\tilde{k}l_z}\left[E_1(-i\tilde{k}l_z + ik_0 l_z) - E_1(-i\tilde{k}l_z)\right]$$

$$+ \frac{(i\tilde{k}l_z + 1)}{4\tilde{k}}\, e^{i\tilde{k}l_z}\left[E_1(\,i\tilde{k}l_z + ik_0 l_z) - E_1(\,i\tilde{k}l_z\,)\right] \qquad \text{(F3)}$$

Fourth Integral

Integrating by parts, we find

$$\int_{k_0}^{\infty} ds\, \frac{s\,(s^2 - k_0^2)^{1/2}\, e^{-(s^2 - k_0^2)^{1/2} l_z}}{(s^2 - k_0^2 + \tilde{k}^2)^2} = \int_0^{\infty} dx\, \frac{x^2\, e^{-x\,l_z}}{(x^2 + \tilde{k}^2)^2} = \int_0^{\infty} dx\, \frac{e^{-x\,l_z}\,(1 - x\,l_z)}{2(x^2 + \tilde{k}^2)}$$

Recall two known integrals [78]:

$$\int dx\, \frac{e^{x}}{(x^2 + a^2)} = -\frac{1}{a}\,\mathrm{Im}\left[e^{ia}\,E_1(-x+ia)\right]$$

$$\int dx\, \frac{x\,e^{x}}{(x^2 + a^2)} = -\,\mathrm{Re}\left[e^{ia}\,E_1(-x+ia)\right] \qquad a > 0$$

Therefore, we have

$$\int_{k_0}^{\infty} ds\, \frac{s\,(s^2 - k_0^2)^{1/2}\, e^{-(s^2 - k_0^2)^{1/2} l_z}}{(s^2 - k_0^2 + \tilde{k}^2)^2} = -\frac{\mathrm{Im}\left[e^{i\tilde{k}l_z}\,E_1(i\tilde{k}l_z)\right]}{2\tilde{k}} - \frac{l_z\,\mathrm{Re}\left[e^{i\tilde{k}l_z}\,E_1(i\tilde{k}l_z)\right]}{2} \qquad \text{(F4)}$$

APPENDIX G

In this appendix, we will derive a numerically efficient simplification of a double integral that appears frequently in this work:

$$I = \int_0^{\Delta} dx \int_0^{\Delta} dx' \cos\left(\frac{\pi x}{\Delta}\right) \cos\left(\frac{\pi x'}{\Delta}\right) \frac{e^{-ik_0\left((x-x')^2+\delta^2\right)^{1/2}}}{\left((x-x')^2+\delta^2\right)^{1/2}}$$

$$= \frac{1}{2} \int_0^{\Delta} dx \int_0^{\Delta} dx' \left[\cos\frac{\pi(x+x')}{\Delta} + \cos\frac{\pi(x-x')}{\Delta}\right] \frac{e^{-ik_0\left((x-x')^2+\delta^2\right)^{1/2}}}{\left((x-x')^2+\delta^2\right)^{1/2}} \tag{G1}$$

The double integration and the situations when δ is much smaller than Δ present unnecessary numerical difficulties that are easy to remove. Let's define two new variables, p and p' as follows

$$\begin{aligned} p &= x - x' \\ p' &= x + x' \end{aligned} \tag{G2}$$

Thus,

$$\begin{aligned} x &= \frac{p + p'}{2} \\ x' &= \frac{p' - p}{2} \end{aligned} \tag{G3}$$

The integration domain is shown in Fig. $G1$. The Jacobian determinant of the transformation is given by [79]:

$$\frac{\partial(x,x')}{\partial(p,p')} = 1/2 \tag{G4}$$

Thus we can integrate with respect to the p' variable,

$$I = \frac{1}{4} \int_{-\Delta}^{0} dp \int_{-p}^{2\Delta+p} dp' \cos\frac{\pi p'}{\Delta} \frac{e^{-ik_0(p^2+\delta^2)^{1/2}}}{(p^2+\delta^2)^{1/2}} + \frac{1}{4} \int_0^{\Delta} dp \int_p^{2\Delta-p} dp' \cos\frac{\pi p'}{\Delta} \frac{e^{-ik_0(p^2+\delta^2)^{1/2}}}{(p^2+\delta^2)^{1/2}}$$

$$+ \frac{1}{4} \int_{-\Delta}^{0} dp \int_{-p}^{2\Delta+p} dp' \cos\frac{\pi p}{\Delta} \frac{e^{-ik_0(p^2+\delta^2)^{1/2}}}{(p^2+\delta^2)^{1/2}} + \frac{1}{4} \int_0^{\Delta} dp \int_p^{2\Delta-p} dp' \cos\frac{\pi p}{\Delta} \frac{e^{-ik_0(p^2+\delta^2)^{1/2}}}{(p^2+\delta^2)^{1/2}}$$

$$= \frac{\Delta}{2\pi} \int_{-\Delta}^{0} dp \sin\frac{\pi p}{\Delta} \frac{e^{-ik_0(p^2+\delta^2)^{1/2}}}{(p^2+\delta^2)^{1/2}} - \frac{\Delta}{2\pi} \int_0^{\Delta} dp \sin\frac{\pi p}{\Delta} \frac{e^{-ik_0(p^2+\delta^2)^{1/2}}}{(p^2+\delta^2)^{1/2}}$$

$$+ \int_0^{\Delta} dp\,(\Delta - p)\cos\frac{\pi p}{\Delta} \frac{e^{-ik_0(p^2+\delta^2)^{1/2}}}{(p^2+\delta^2)^{1/2}} \tag{G5}$$

Or,

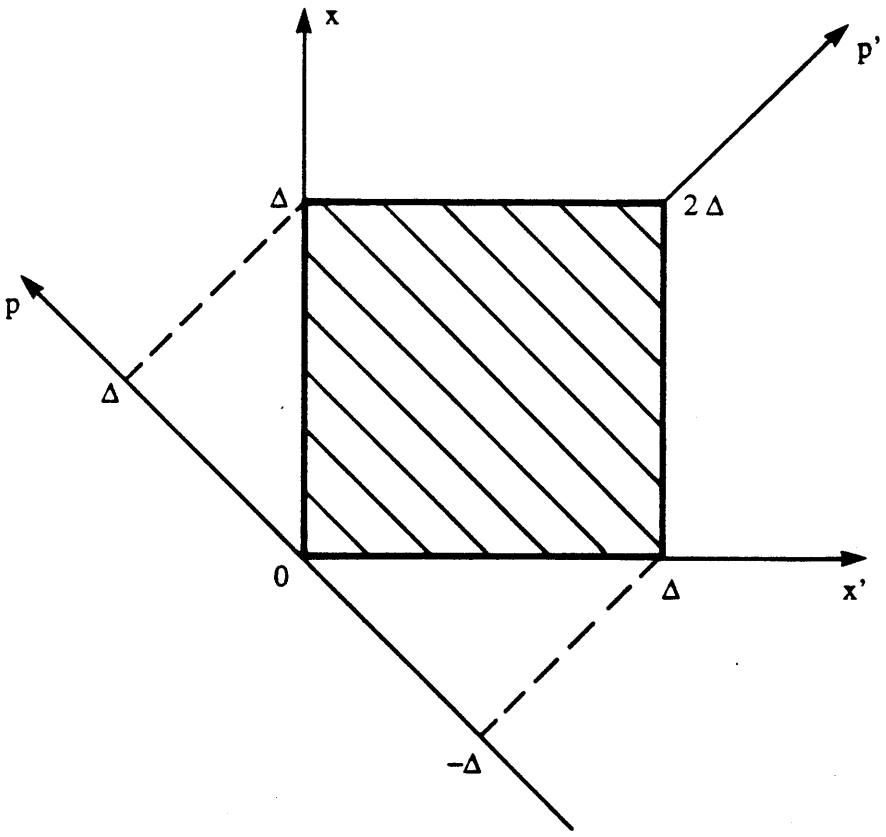

Fig. G1. Integration domain.

$$I = \int_0^{\Delta} dp \left[(\Delta - p)\cos\frac{\pi p}{\Delta} - \frac{\Delta}{\pi}\sin\frac{\pi p}{\Delta}\right] \frac{e^{-ik_0(p^2+\delta^2)^{1/2}}}{(p^2+\delta^2)^{1/2}} \tag{G6}$$

When δ is much smaller than Δ, it is useful to substract the singular behavior at $p = 0$ and to compute it separately. Thus,

$$I = \int_0^{\Delta} dp \frac{\left[(\Delta - p)\cos\frac{\pi p}{\Delta} - \frac{\Delta}{\pi}\sin\frac{\pi p}{\Delta}\right] e^{-ik_0(p^2+\delta^2)^{1/2}} - \Delta}{(p^2+\delta^2)^{1/2}} + \Delta\sinh^{-1}(\Delta/\delta) \tag{G7}$$

The same technique yields the simpler but equally useful result

$$\int_0^{\Delta} dx \int_0^{\Delta} dx' \frac{e^{-ik_0\left((x-x')^2+\delta^2\right)^{1/2}}}{\left((x-x')^2+\delta^2\right)^{1/2}} = 2\int_0^{\Delta} dp\,(\Delta - p)\frac{e^{-ik_0(p^2+\delta^2)^{1/2}}}{(p^2+\delta^2)^{1/2}} \tag{G8}$$

APPENDIX H

In this appendix, we outline the calculations needed for the rectangular patch.

Method 1 (Method presented in this report)

1. Estimate the resonant frequency

$$f = \frac{1}{2l_x(\epsilon_0\epsilon_r\mu_0\mu_r)^{1/2}}$$

2. Calculate the "ideal" cavity wavenumber $\tilde{k}_{10} = \pi / l_x$
3. Calculate the free-space wavenumber $k_0 = 2\pi f\ (\epsilon_0\mu_0)^{1/2}$
4. Calculate I_{11}, I_{13}, I_{22}, I_{24}, J_{11} and J_{13} from equations (63) or (64), (65) - (67), (72) and (73)
5. Calculate the complex wavenumber k_{10} from (75)
6. Calculate the resonant frequency

$$f = \mathrm{Re}\left[\frac{k_{10}}{2\pi(\epsilon_0\epsilon_r\mu_0\mu_r)^{1/2}}\right]$$

7. Calculate the Q-factor from (57)
8. Repeat steps 3 to 7 with the better estimate of the resonant frequency given in step 6.

Method 2 (Kuester, Johnk and Chang's analysis [29])

1. Calculate δ_ϵ and δ_μ from equations (40) and (42).
2. Calculate $Q_0(-\delta_\epsilon)$ and $Q_0(\delta_\mu)$ from equation (39)
3. Calculate the index of refraction $n = (\epsilon_r\mu_r)^{1/2}$
4. Calculate the effective refractive index

$$n_{eff} = n -$$

$$\frac{d}{l_y\pi n}\left[2n^2\left(Q_0(-\delta_\epsilon) - Q_0(\delta_\mu)\right) + (1-n^2)\,\mu_r\left(\ln\left[\frac{\pi d}{nl_x}(n^2-1)^{1/2}\right] + \gamma - 1\right)\right]$$

5. Calculate the edge extension

$$\Delta h = -\frac{d}{\pi}\left(\frac{\ln(\pi d/nl_x) + \gamma - 1}{\epsilon_r} + 2Q_0(-\delta_\epsilon) - \ln(2\pi)\right)$$

6. Calculate the resonant frequency

$$f = \frac{1}{2n_{eff}\,(l_x + 2\Delta h)(\epsilon_0\mu_0)^{1/2}}$$

7. Calculate the Q-factor

$$Q = \frac{n^3 l_x^2}{2n_{eff}\,d\,(l_x + 2\Delta h)}$$

Method 3 (Carver's modal analysis [27])

1. Estimate an effective dielectric constant

$$\epsilon_e = \frac{\epsilon_r + 1}{2} + \frac{\epsilon_r - 1}{2}\left[1 + \frac{10d}{l_y}\right]^{-1/2}$$

2. Calculate the edge extension parameter

$$\frac{\Delta l}{d} = 0.412\left[\frac{\epsilon_e + 0.3}{\epsilon_e - 0.258}\right]\left[\frac{l_y/d + 0.262}{l_y/d + 0.813}\right]$$

3. Estimate the free-space wavelength $\lambda_0 = 2l_x\,(\epsilon_r)^{1/2}$
4. Calculate the wall susceptance $B = 0.01668\,(\Delta l\,\epsilon_e\,l_y)\,/\,(d\lambda_0)$
5. Calculate the wall conductance $G = 0.00836\,l_y\,/\,\lambda_0$
6. Calculate the aspect factor

$$F = 0.7747 + 0.5977\,(l_y/l_x - 1) - 0.1638\,(l_y/l_x - 1)^2$$

7. Calculate the impedance parameter

$$\kappa = \frac{240\,i\pi^2 d}{\lambda_0 l_y}(G + iB)\,F\,l_x$$

8. Calculate the eigenvalue shift factor with 4 iterations using $\Delta_0 = 0$

$$\Delta_{p+1} = \frac{2\kappa(\pi - \Delta_p)}{\kappa^2 + 2\Delta_p\pi - \Delta_p^2 - \pi^2} - \frac{\Delta_p^3}{3}$$

9. Calculate the complex wavenumber $k_{10} = (\pi - \Delta_4)\,/\,l_x$
10. Calculate the resonant frequency

$$f = \frac{\mathrm{Re}[k_{10}]}{2\pi(\epsilon_0\epsilon_r\mu_0)^{1/2}}$$

11. Calculate the Q-factor from equation (57).

APPENDIX I

In this appendix, we calculate three coupling integrals needed for the dominant mode solution of the circular patch.

Integral I_C

$$I_C = \oint_P dl \oint_P dl' \, [\bar{a}_l \cdot \bar{a}_{l'}] \, \tilde{V}(l) \, \tilde{V}(l') \, G_d(l,l')$$

$$= \left[dR \, J_1(j'_{1,1}) \right]^2 \int_0^{2\pi} d\phi \int_0^{2\pi} d\phi' \cos(\phi - \phi') \cos\phi \cos\phi' \, \frac{e^{-ik_0 \left(4R^2 \sin^2(\phi - \phi')/2 + d^2\right)^{1/2}}}{\left(4R^2 \sin^2(\phi - \phi')/2 + d^2\right)^{1/2}} \tag{I1}$$

Let's make the change of variable $\alpha = \phi' - \phi$, thus,

$$I_C = \left[dR \, J_1(j'_{1,1}) \right]^2 \int_0^{2\pi} d\phi \, \cos\phi \int_{\phi}^{2\pi+\phi} d\alpha \, \cos\alpha \cos(\phi + \alpha) \, \frac{e^{-ik_0 \left(4R^2 \sin^2(\alpha/2) + d^2\right)^{1/2}}}{\left(4R^2 \sin^2(\alpha/2) + d^2\right)^{1/2}}$$

The integration on the α variable is over a full period. We can thus shift the limits over any period and, in particular, from 0 to 2π. Expanding $\cos(\phi + \alpha)$,

$$I_C = \left[dR \, J_1(j'_{1,1}) \right]^2$$

$$\cdot \int_0^{2\pi} d\phi \cos\phi \int_0^{2\pi} d\alpha \, \cos\alpha (\cos\alpha \cos\phi - \sin\alpha \sin\phi) \, \frac{e^{-ik_0 \left(4R^2 \sin^2(\alpha/2) + d^2\right)^{1/2}}}{\left(4R^2 \sin^2(\alpha/2) + d^2\right)^{1/2}} \tag{I2}$$

The above result simplifies immediately to

$$I_C = 2\pi \left[dR \, J_1(j'_{1,1}) \right]^2 \int_0^{\pi} d\alpha \, \cos^2\alpha \, \frac{e^{-ik_0 \left(4R^2 \sin^2(\alpha/2) + d^2\right)^{1/2}}}{\left(4R^2 \sin^2(\alpha/2) + d^2\right)^{1/2}} \tag{I3}$$

Since, by hypothesis, $(k_0 d) << 1$, we need to isolate the singularity of the integrand for small values of α. Therefore, we write

$$I_C = 2\pi \left[dR \, J_1(j'_{1,1}) \right]^2$$

$$\cdot \left[\int_0^{\pi} \frac{d\alpha}{\left(4R^2 \sin^2(\alpha/2) + d^2\right)^{1/2}} + \int_0^{\pi} d\alpha \, \frac{\cos^2\alpha \, e^{-ik_0 \left(4R^2 \sin^2(\alpha/2) + d^2\right)^{1/2}} - 1}{\left(4R^2 \sin^2(\alpha/2) + d^2\right)^{1/2}} \right] \tag{I4}$$

The second integral, because of the smooth integrand, is easily integrated numerically. The first integral, as shown below, can be computed in closed form. First, perform the change of variable $\theta = \alpha/2$. We obtain

$$\int_0^{\pi} \frac{d\alpha}{\left(4R^2 \sin^2(\alpha/2) + d^2\right)^{1/2}} = \int_0^{\pi/2} \frac{2 \, d\theta}{\left(4R^2 \sin^2\theta + d^2\right)^{1/2}} = \int_0^{\pi/2} \frac{2 \, d\theta}{\left(4R^2 \cos^2\theta + d^2\right)^{1/2}}$$

$$= \frac{2}{(4R^2+d^2)^{1/2}} \int_0^{\pi/2} \frac{d\theta}{\left(1-\frac{4R^2\sin^2\theta}{4R^2+d^2}\right)^{1/2}} = \frac{2}{(4R^2+d^2)^{1/2}} \mathbf{K}\left(\frac{4R^2}{4R^2+d^2}\right) \tag{I5}$$

where **K** is the complete elliptic integral of the first kind [57]. Finally,

$$I_C = 2\pi \left[dR\, \mathbf{J}_1(j'_{1,1}) \right]^2 \left[\frac{2\,\mathbf{K}\left(\frac{4R^2}{4R^2+d^2}\right)}{(4R^2+d^2)^{1/2}} + \int_0^{\pi} d\alpha\, \frac{\cos^2\alpha\; e^{-ik_0\left(4R^2\sin^2(\alpha/2)+d^2\right)^{1/2}} - 1}{\left(4R^2\sin^2(\alpha/2)+d^2\right)^{1/2}} \right] \tag{I6}$$

Integral J_C

$$J_C = \oint_P dl \oint_P dl'\, \frac{\partial \tilde{V}}{\partial l}\, \frac{\partial \tilde{V}}{\partial l'}\, G_d(l,l')$$

$$= d^2 \mathbf{J}_1^2(j'_{1,1}) \int_0^{2\pi} d\phi\, \sin\phi \int_0^{2\pi} d\phi'\, \sin\phi'\, \frac{e^{-ik_0\left(4R^2\sin^2(\phi-\phi')/2+d^2\right)^{1/2}}}{\left(4R^2\sin^2(\phi-\phi')/2+d^2\right)^{1/2}} \tag{I7}$$

Let's make the change of variable $\alpha = \phi' - \phi$. Thus,

$$J_C = d^2\, \mathbf{J}_1^2(j'_{1,1}) \int_0^{2\pi} d\phi\, \sin\phi \int_{\phi}^{2\pi+\phi} d\alpha\, \sin(\phi+\alpha)\, \frac{e^{-ik_0\left(4R^2\sin^2(\alpha/2)+d^2\right)^{1/2}}}{\left(4R^2\sin^2(\alpha/2)+d^2\right)^{1/2}} \tag{I8}$$

$$= d^2\, \mathbf{J}_1^2(j'_{1,1}) \int_0^{2\pi} d\phi\, \sin^2\phi \int_0^{2\pi} d\alpha\, \cos\alpha\, \frac{e^{-ik_0\left(4R^2\sin^2(\alpha/2)+d^2\right)^{1/2}}}{\left(4R^2\sin^2(\alpha/2)+d^2\right)^{1/2}}$$

$$= 2\pi d^2\, \mathbf{J}_1^2(j'_{1,1}) \int_0^{\pi} d\alpha\, \cos\alpha\, \frac{e^{-ik_0\left(4R^2\sin^2(\alpha/2)+d^2\right)^{1/2}}}{\left(4R^2\sin^2(\alpha/2)+d^2\right)^{1/2}} \tag{I9}$$

We can take care of the singularity of the integrand in the same way as for the integral I_C above. Finally, we have

$$J_C = 2\pi d^2\, \mathbf{J}_1^2(j'_{1,1}) \left[\frac{2\mathbf{K}\left(\frac{4R^2}{4R^2+d^2}\right)}{(4R^2+d^2)^{1/2}} + \int_0^{\pi} d\alpha\, \frac{\cos\alpha\; e^{-ik_0\left(4R^2\sin^2(\alpha/2)+d^2\right)^{1/2}} - 1}{\left(4R^2\sin^2(\alpha/2)+d^2\right)^{1/2}} \right] \tag{I10}$$

Integral I_S

$$I_S = \int_{S_C} ds\, \tilde{V}^2 = d^2 \int_0^{2\pi} d\phi\, \cos^2\phi \int_0^{R} d\rho\, \rho\, \mathbf{J}_1^2\left(\frac{j'_{1,1}\rho}{R}\right) \tag{I11}$$

Recall the integral [80]:

$$\int dz\; z\, \mathbf{J}_1^2(az) = \frac{z^2}{2}\left[\left(1-\frac{1}{a^2z^2}\right)\mathbf{J}_1^2(az) + \mathbf{J}_1'^2(az)\right] \tag{I12}$$

It follows immediately that

$$\int_0^R d\rho\ \rho\ \mathrm{J}_1^2\left(\frac{j'_{1,1}\rho}{R}\right) = \frac{R^2}{2}\left(1 - \frac{1}{j'^2_{1,1}}\right)\mathrm{J}_1^2(j'_{1,1}) \tag{I13}$$

And therefore,

$$I_S = \frac{\pi d^2 R^2}{2}\left(1 - \frac{1}{j'^2_{1,1}}\right)\mathrm{J}_1^2(j'_{1,1}) \tag{I14}$$

APPENDIX J

In this appendix, we outline the calculations needed for the circular patch. Note that the step 5 in Carver's method has been corrected from the expressions found in [27] and [55].

Method 1 (Method presented in this report)

1. Estimate the resonant frequency

$$f = \frac{j'_{1,1}}{2\pi R(\epsilon_0\epsilon_r\mu_0\mu_r)^{1/2}}$$

2. Calculate the "ideal" cavity wavenumber $\tilde{k}_{11} = j'_{1,1} / R$
3. Calculate the free-space wavenumber $k_0 = 2\pi f\ (\epsilon_0\mu_0)^{1/2}$
4. Calculate I_C, J_C and I_S from equations (87), (88) and (89)
5. Calculate the line integrals (90) and (91)
6. Calculate the complex wavenumber k_{11} from (81)
7. Calculate the resonant frequency

$$f = \mathrm{Re}\left[\frac{k_{11}}{2\pi(\epsilon_0\epsilon_r\mu_0\mu_r)^{1/2}}\right]$$

8. Calculate the Q-factor from equation (57)
9. Repeat steps 3 to 8 with the better estimate of the resonant frequency given in step 7.

Method 2 (Carver's modal analysis [27])

1. Estimate the free-space wavelength $\lambda_0 = 2\pi R\,(\epsilon_r)^{1/2} / j'_{1,1}$
2. Calculate the wall susceptance $B = 0.00834\ \pi R\,\epsilon_r\ / \lambda_0$
3. Calculate the wall conductance $G = 0.01254\ \pi R\ / \lambda_0$
4. Calculate the edge impedance parameter

$$\alpha = \frac{120\,i\pi d}{R\lambda_0}\,(G + iB)$$

5. Calculate the eigenvalue shift factor with five iterations using $\Delta_0 = 0$

$$\Delta_{p+1} = \frac{\left[1.8410969 + 4.0260952\,\Delta_p^2\right](1 - \alpha R) - 1.84118}{3.3263839(1 - \alpha R) - 1}$$

6. Calculate the complex wavenumber $k_{11} = (1.84118 - \Delta_5)/R$

7. Calculate the resonant frequency

$$f = \frac{\mathrm{Re}[k_{11}]}{2\pi(\epsilon_0\epsilon_r\mu_0)^{1/2}}$$

8. Calculate the Q-factor from (57).